EPFL

EDMI Microsystems and Microelectronics

MICRO-614: Electrochemical Nano-Bio-Sensing and Bio/CMOS interfaces

Lecture #7

Checking Probes-layer quality (RM+SPR+SEM+AFM)

Lecture Outline

(Book Bio/CMOS: Chapter' paragraphs § 5.2.1-2)

- Resonant Mirror
- Surface Plasmon Resonance

To monitor the self-assembly process

- Transmission Electron Microscopy
- Scanning Electron Microscopy
- Atomic Force Microscopy
- Scanning Tunneling Microscopy

To check the film quality

Three-layers Reflection

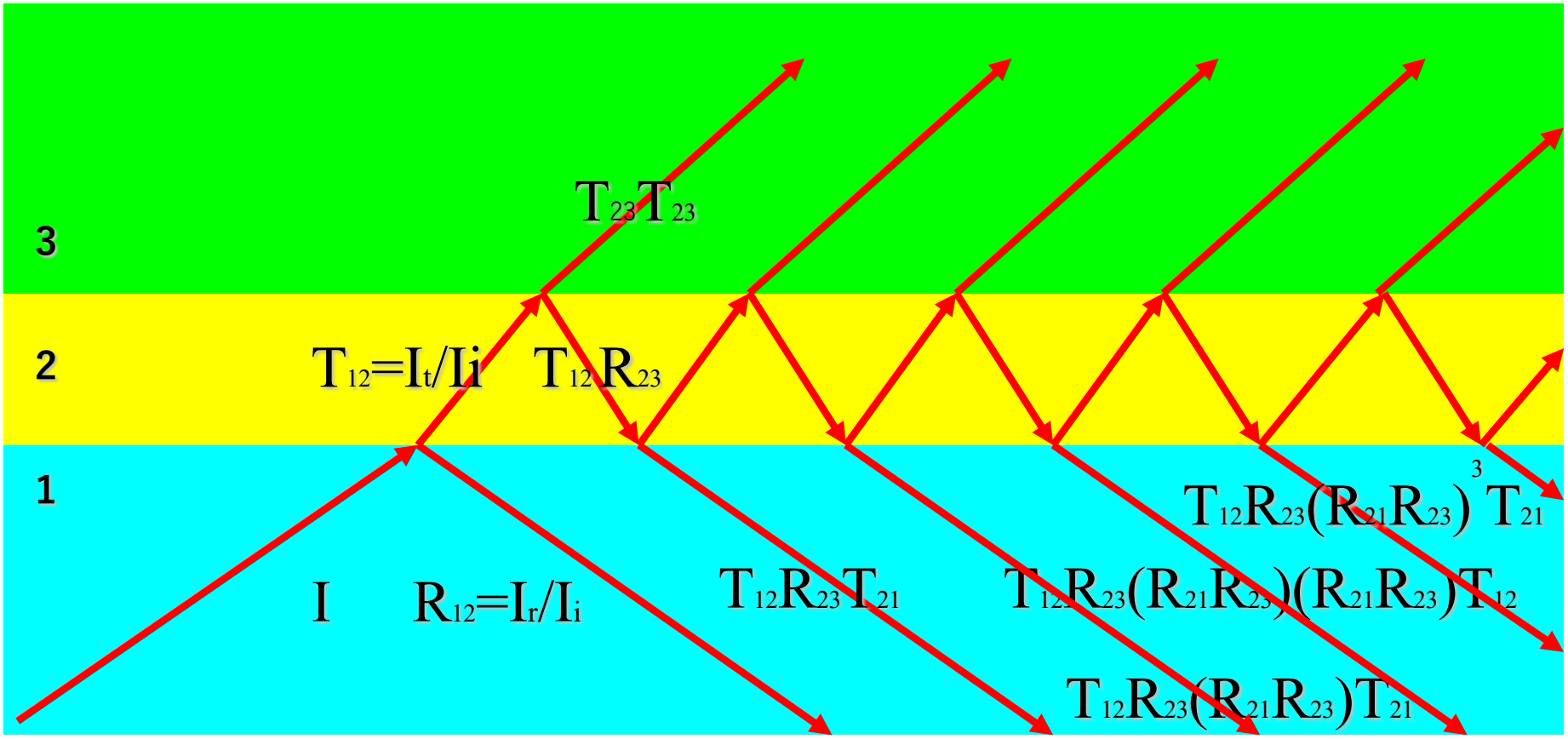

$$R = R_{12} + T_{12}R_{23}T_{21} + T_{12}R_{23}T_{21}(R_{21}R_{23}) + T_{12}R_{23}T_{21}(R_{21}R_{23})^2 + \ldots$$

Three-layers Reflection

$$R = R_{12} + T_{12}R_{23}T_{21} + T_{12}R_{23}T_{21}(R_{21}R_{23}) + T_{12}R_{23}T_{21}(R_{21}R_{23})^2 + \ldots$$

$$R = R_{12} + \sum_{n=0}^{\infty} T_{12}R_{23}T_{21}(R_{21}R_{23})^n$$

$$R = R_{12} + T_{12}R_{23}T_{21}\sum_{n=0}^{\infty}(R_{21}R_{23})^n$$

By the geometric series

$$\sum_{n=0}^{\infty} x^n = \frac{1}{1-x}$$

$$R = R_{12} + T_{12}R_{23}T_{21}\frac{1}{1-R_{21}R_{23}}$$

The Reflection coefficient and the Electrical Field

$$R = R_{12} + \frac{T_{12} R_{23} T_{21}}{1 - R_{21} R_{23}}$$

$$R_{23} = |r_{23}|^2$$

$$R_{23} = \frac{I_r}{I_i}; r_{23} = \frac{E_r}{E_i}$$

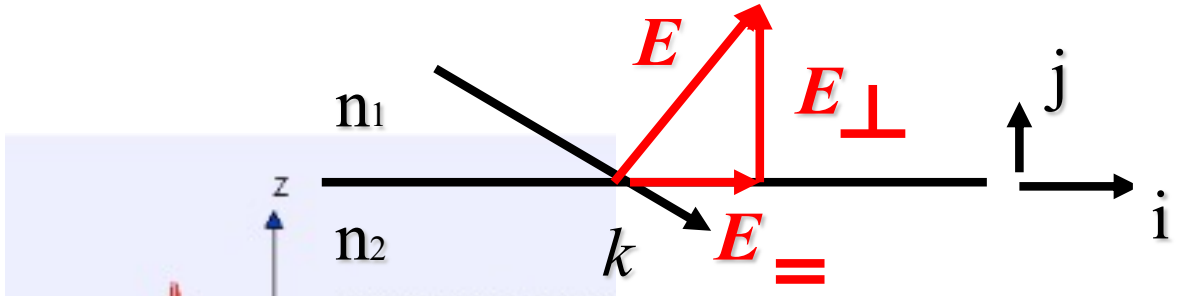

$$\vec{k} = \frac{1}{\sqrt{2}}(\vec{i} + \vec{j})$$

$$\vec{E} = E_{\Rightarrow}\vec{i} + E_{\perp}\vec{j}$$

$$r_{23} \xrightarrow{splitted} r_{\Rightarrow}, r_{\perp}$$

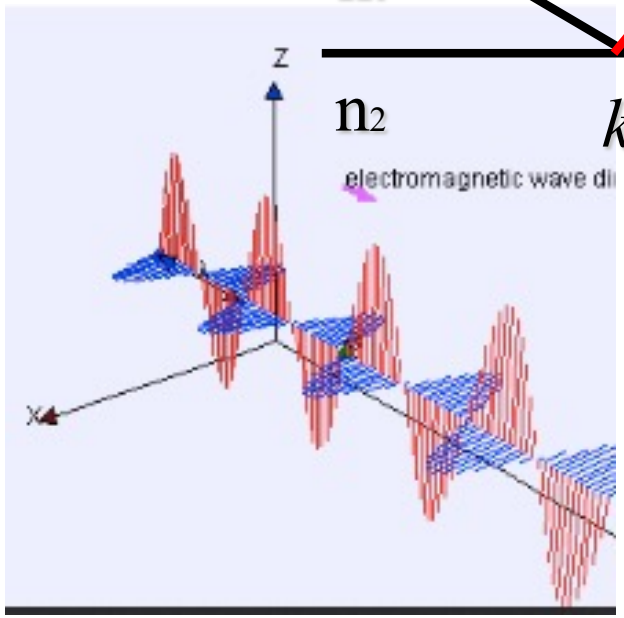

The Fresnel Coefficients

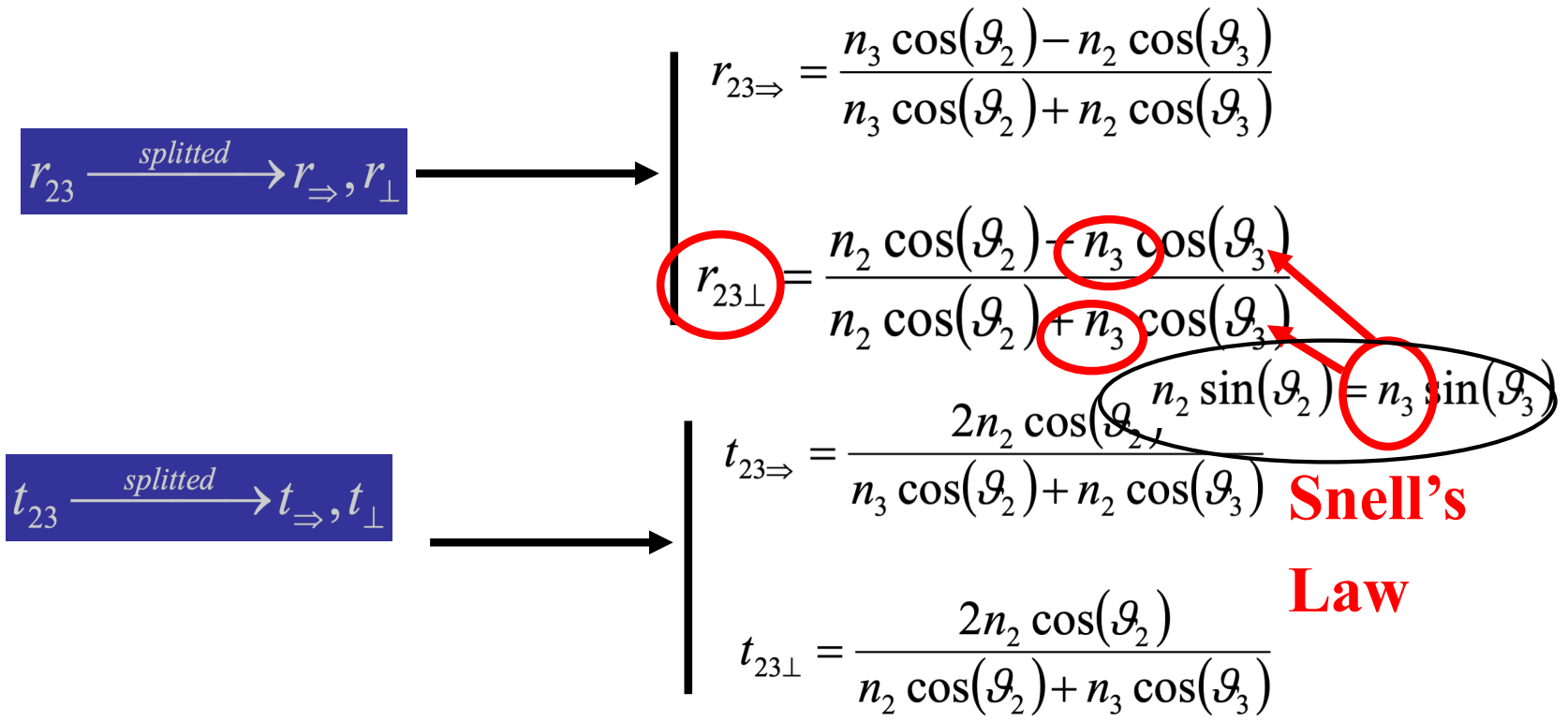

Three-layers Reflection

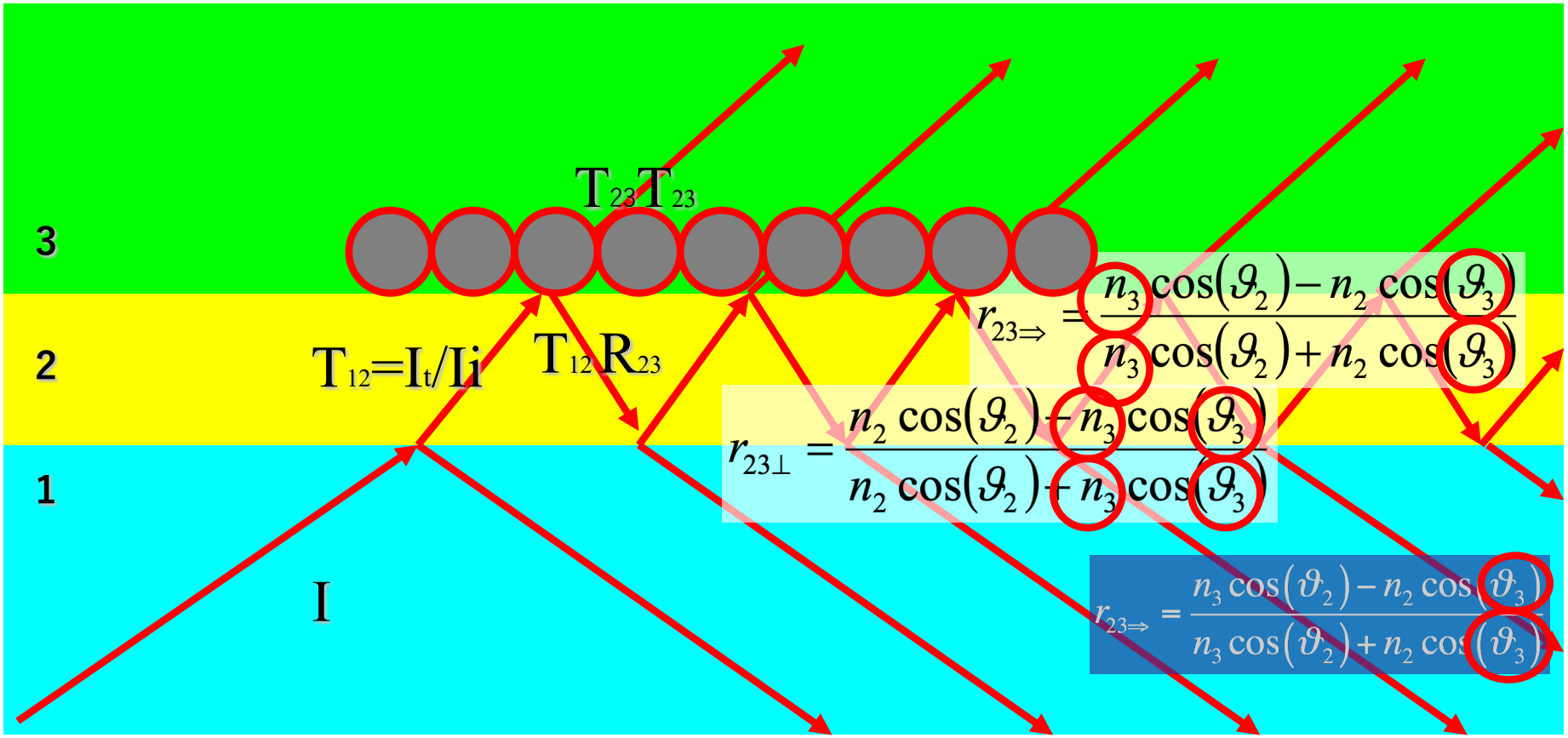

Product

IAsys *plus* Affinity Sensor

Yield Monitoring

Yield = Percentage of covered surface

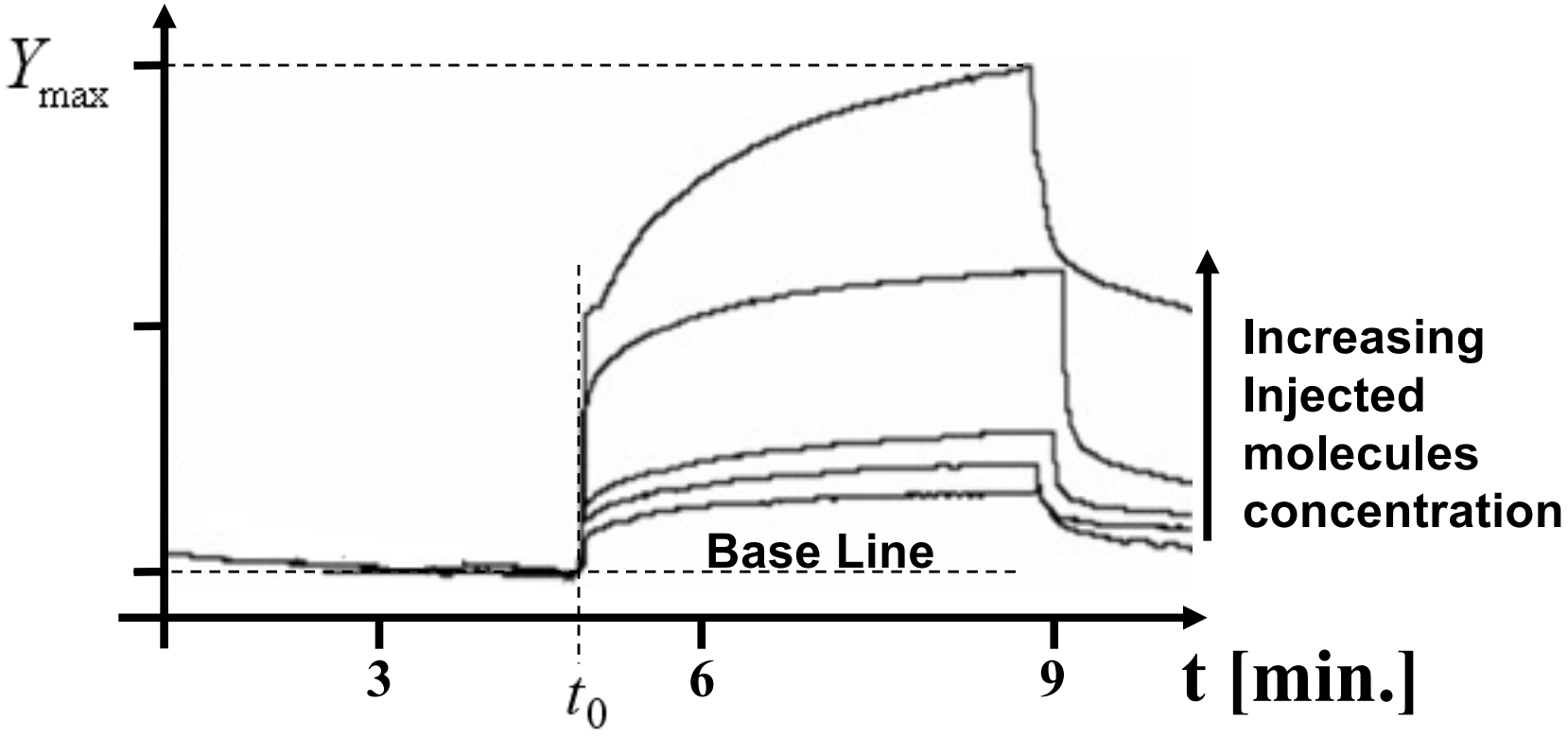

Three-layers Reflection

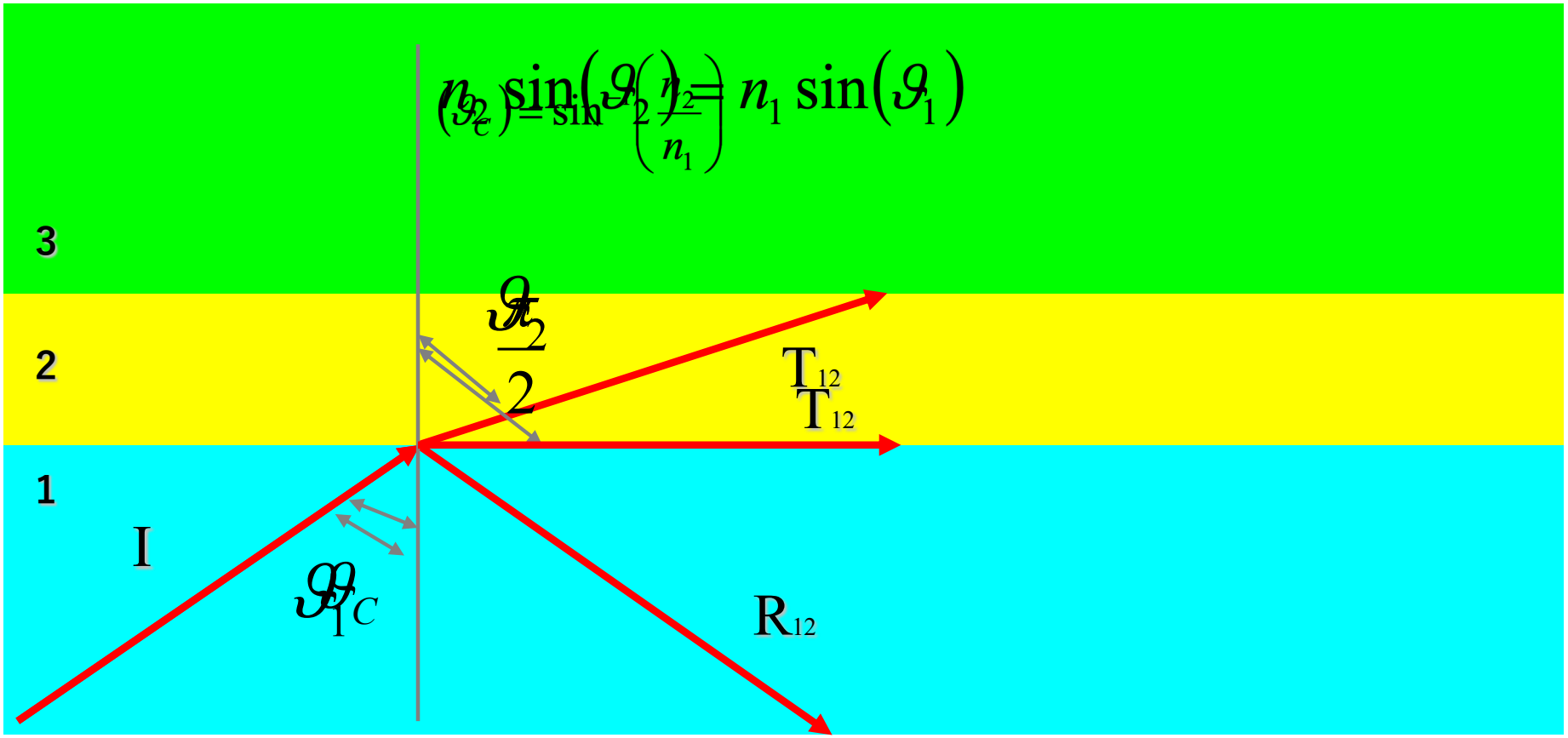

The Propagation along the interface

$$k_{pz} = \sqrt{k_0^2 \varepsilon_p - k_x^2}$$

$$E_t = E_{0t} e^{ik_x x + ik_{pz} z - i\omega t}$$

$$\begin{cases} k_0 = \omega / c = 2\pi / \lambda \\ k_x = k_0 \sqrt{\varepsilon_p} \sin(\vartheta) \\ n_2 = \sqrt{\varepsilon_p \mu_p} \end{cases}$$

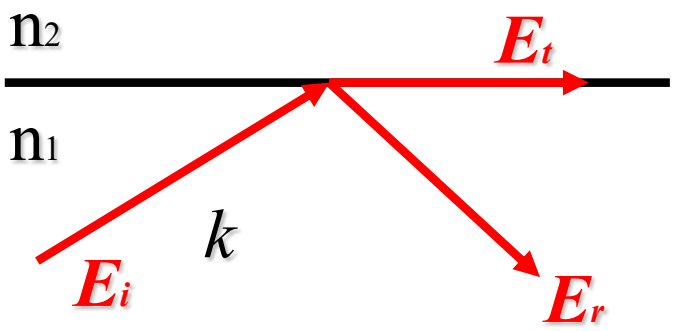

$$E_i = E_{0i} e^{ik_x x + ik_z z - i\omega t} \qquad E_r = E_{0r} e^{ik_x x - ik_z z - i\omega t}$$

The Evanescent wave

$$E_t = E_{0t} e^{ik_x x + ik_{pz} z - i\omega t} \qquad k_{pz} = \sqrt{k_0^2 \varepsilon_p - k_x^2}$$

$$\varepsilon_p \le 0$$

$$E_t = \left(E_{0t} e^{-|k_{pz}| z} \right) e^{ik_x x - i\omega t}$$

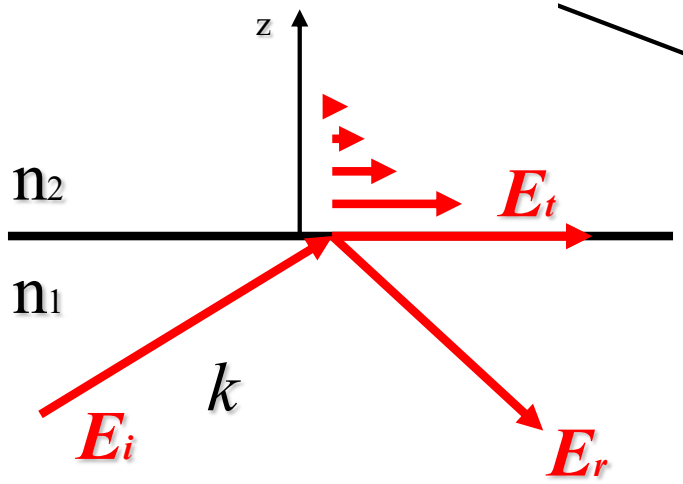

Negative Permeability of metals

Zhang *et al.* J. Opt. Soc. Am. B/Vol. 23, No. 3/March 2006 pag 434

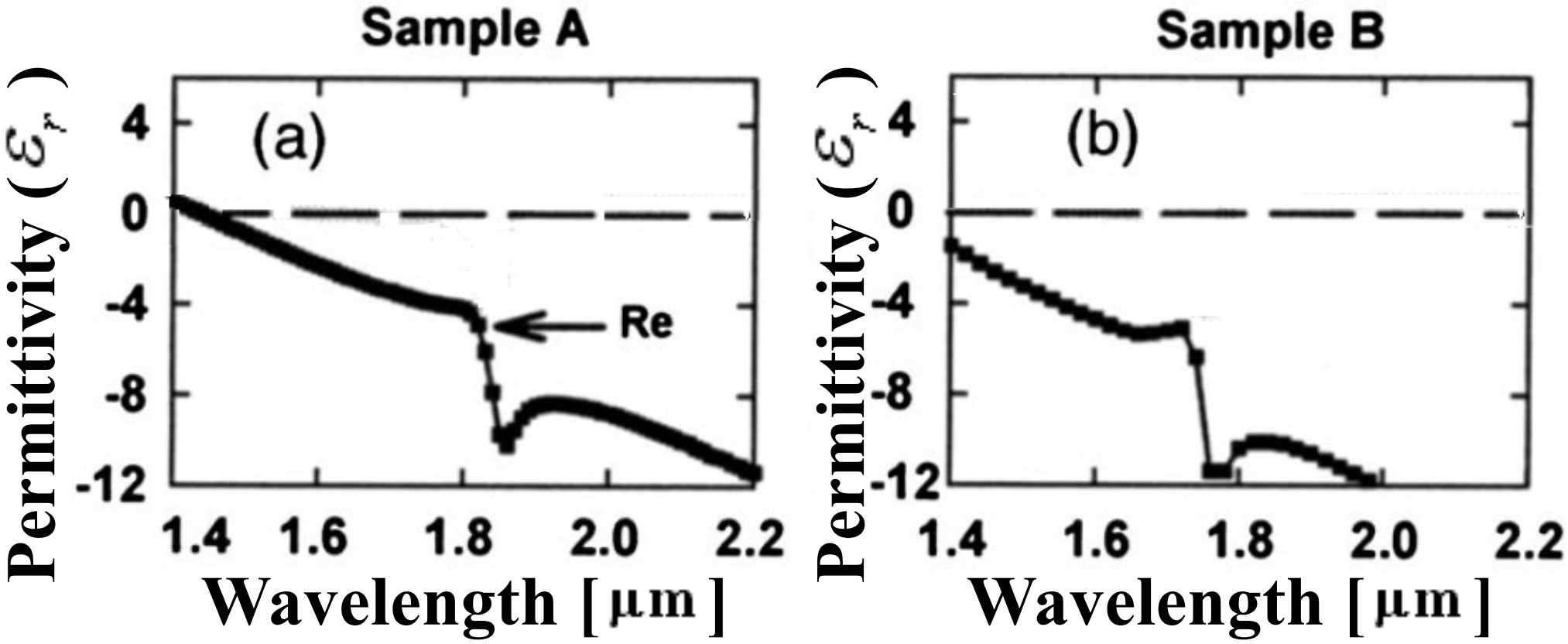

Negative Permittivity in metallic clots

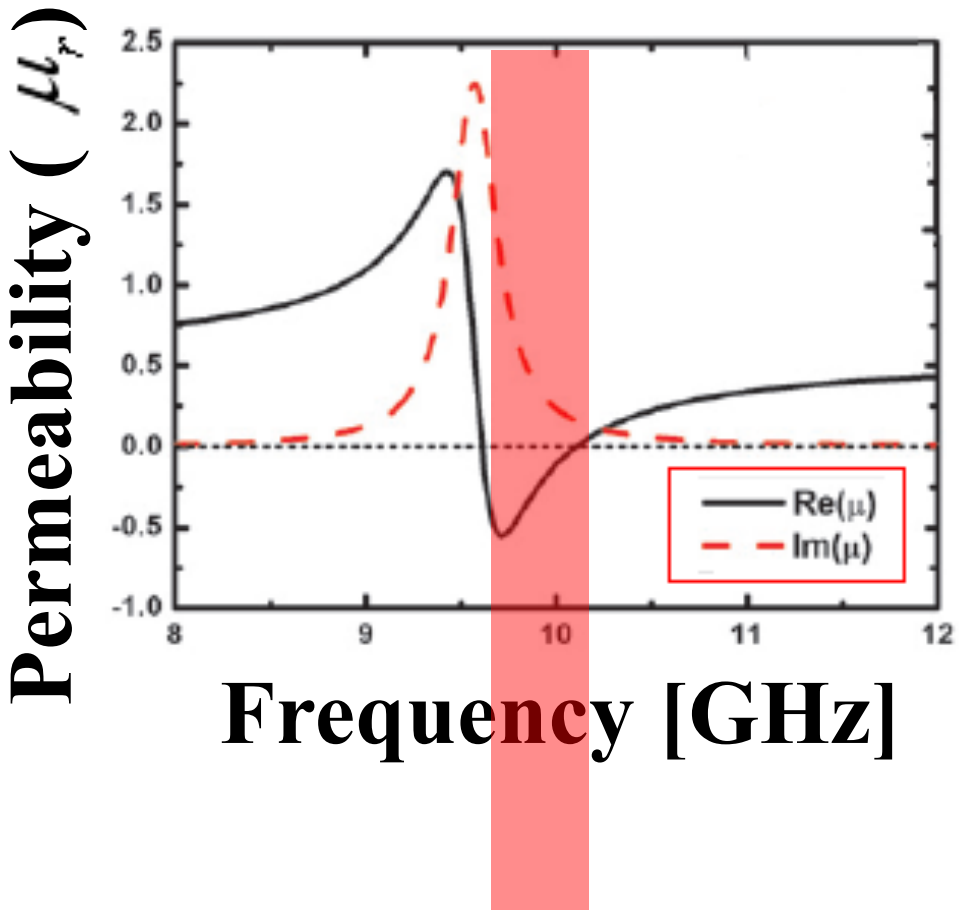

New Journal of Physics **10** (2008) 115039 (15pp)

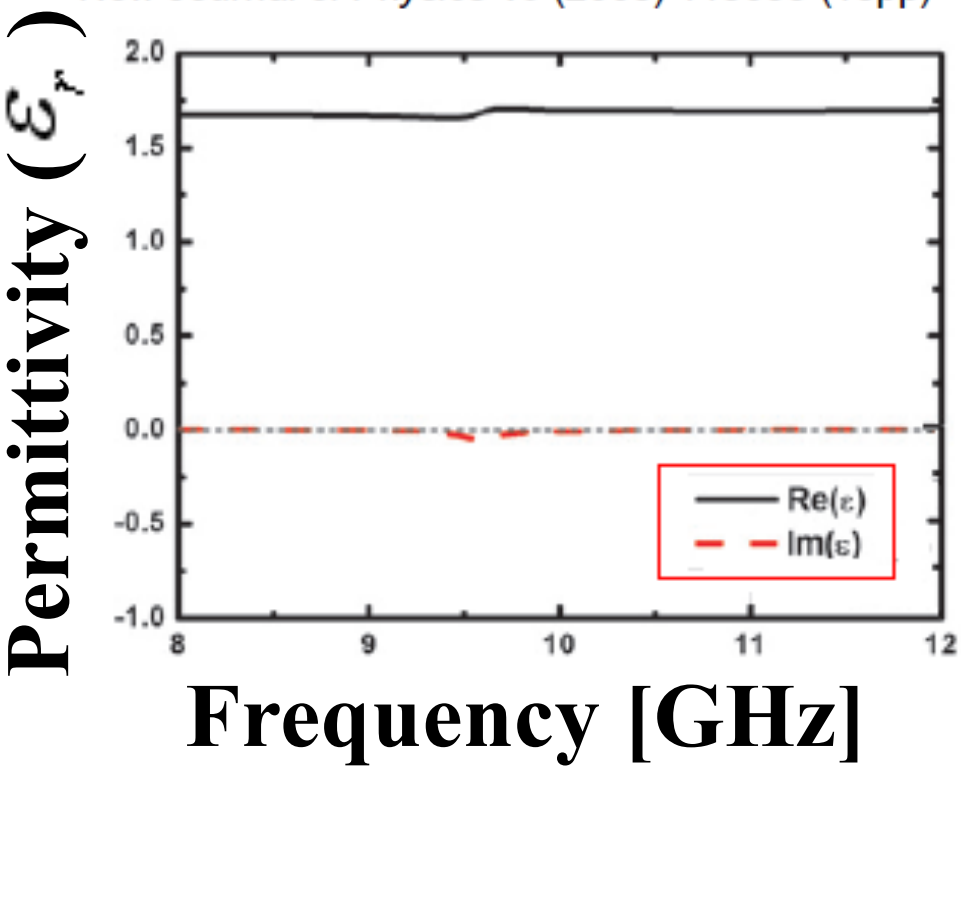

Region of frequencies with negative permeability

Negative dielectric constant

$$E_t = \left(E_{0t} e^{-|k_{pz}|z} \right) e^{ik_x x - i\omega t}$$

$\varepsilon_p \le 0$!

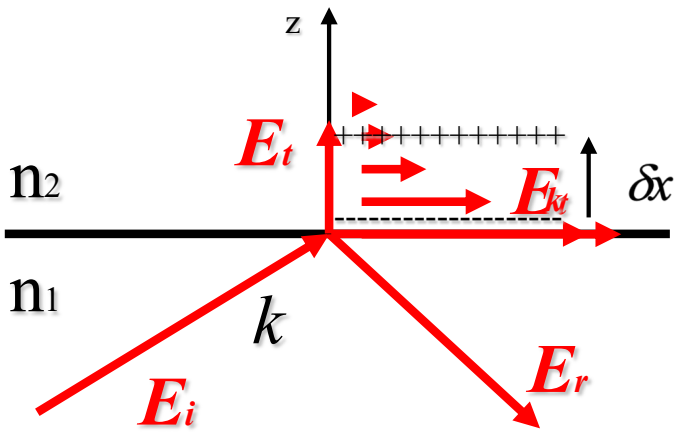

$$F = ma = m\frac{\partial^2 \delta x}{\partial t^2}$$

$$F = eE_t = -eE_{\delta x} = -e\frac{\sigma}{\varepsilon_0}$$

$$F = -e\frac{en_e \delta x}{\varepsilon_0}$$

$$\frac{\partial^2 \delta x}{\partial t^2} + \frac{e^2 n_e \delta x}{m\varepsilon_0} = 0$$

$$\omega_p^2 = \frac{e^2 n_e}{m\varepsilon_0} \leftarrow \frac{\partial^2 \varphi}{\partial t^2} - \frac{e^2 n_e}{m\varepsilon_0}\varphi = 0$$

Electronic Waves

$$\frac{\partial^2 \delta x}{\partial t^2} + \omega_p^2 \delta x = 0 \longrightarrow \delta x = \delta x_0 e^{-i\omega_p t} = \frac{\varepsilon_0 E_{0t} e^{-|k_{pz}| z_p}}{e} e^{-i\omega_p t}$$

The Plasmon!

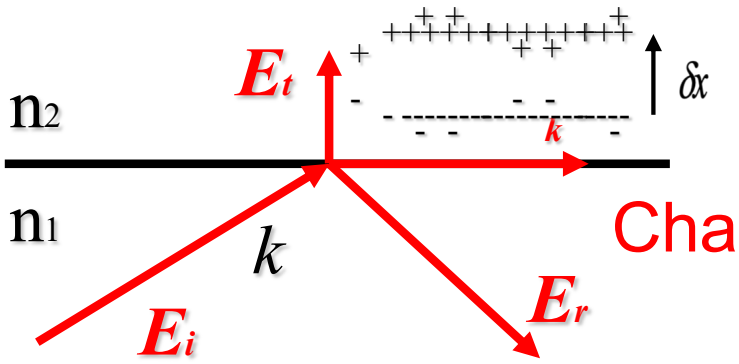

$$\omega_p^2 = \frac{e^2 n_e}{m \varepsilon_0}$$

Characteristic of the metal

$$k_{pz} = \sqrt{k_0^2 \varepsilon_p - k_x^2}$$

Characteristic of the evanescent wave

Simulation of Evanescent wave propagation

410 nm for HeNe laser in glass

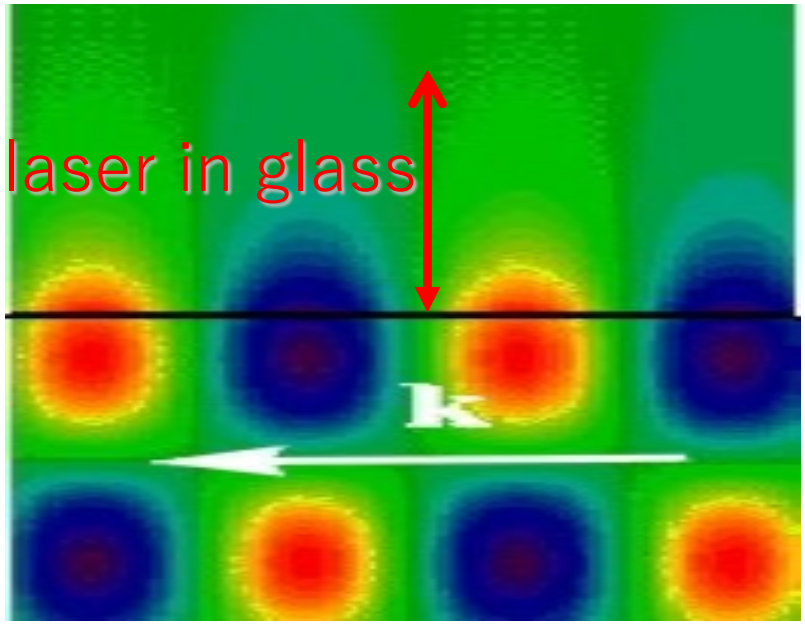

Penetration of the Evanescent Wave

For an amplitude of 1/3 of the value in z=0, we have

$$E_{ot}e^{-|k_{mz}|z} = \frac{1}{3}E_t|_{z=0} = \frac{1}{3}E_{0t} \longrightarrow e^{-|k_{mz}|z} = \frac{1}{3} \approx \frac{1}{e}$$

By extracting z:

$$z = \frac{1}{|k_{mz}|} = \frac{c_0}{2\pi f\sqrt{|\mu_r\varepsilon_r|}} = \frac{\lambda}{\sqrt{|\mu_r\varepsilon_r|}}$$

For gold, with relative magnetic permeability close to one and relative electric permittivity equal to 6.9, we obtain a thickness of

$$z_{gold} = \frac{1}{|k_{mz}|} = \frac{\lambda}{\sqrt{|\mu_r\varepsilon_r|}} = \frac{400\,nm}{\sqrt{6.9\cdot 1}} \approx 152\,nm$$

For nickel, with permeability and permittivity equal to 100 and 10 (respectively), we get:

$$z_{nickel} = \frac{1}{|k_{mz}|} = \frac{\lambda}{\sqrt{|\mu_r\varepsilon_r|}} \approx \frac{400\,nm}{\sqrt{100\cdot 10}} \approx 12\,nm$$

Penetration of the Evanescent Wave

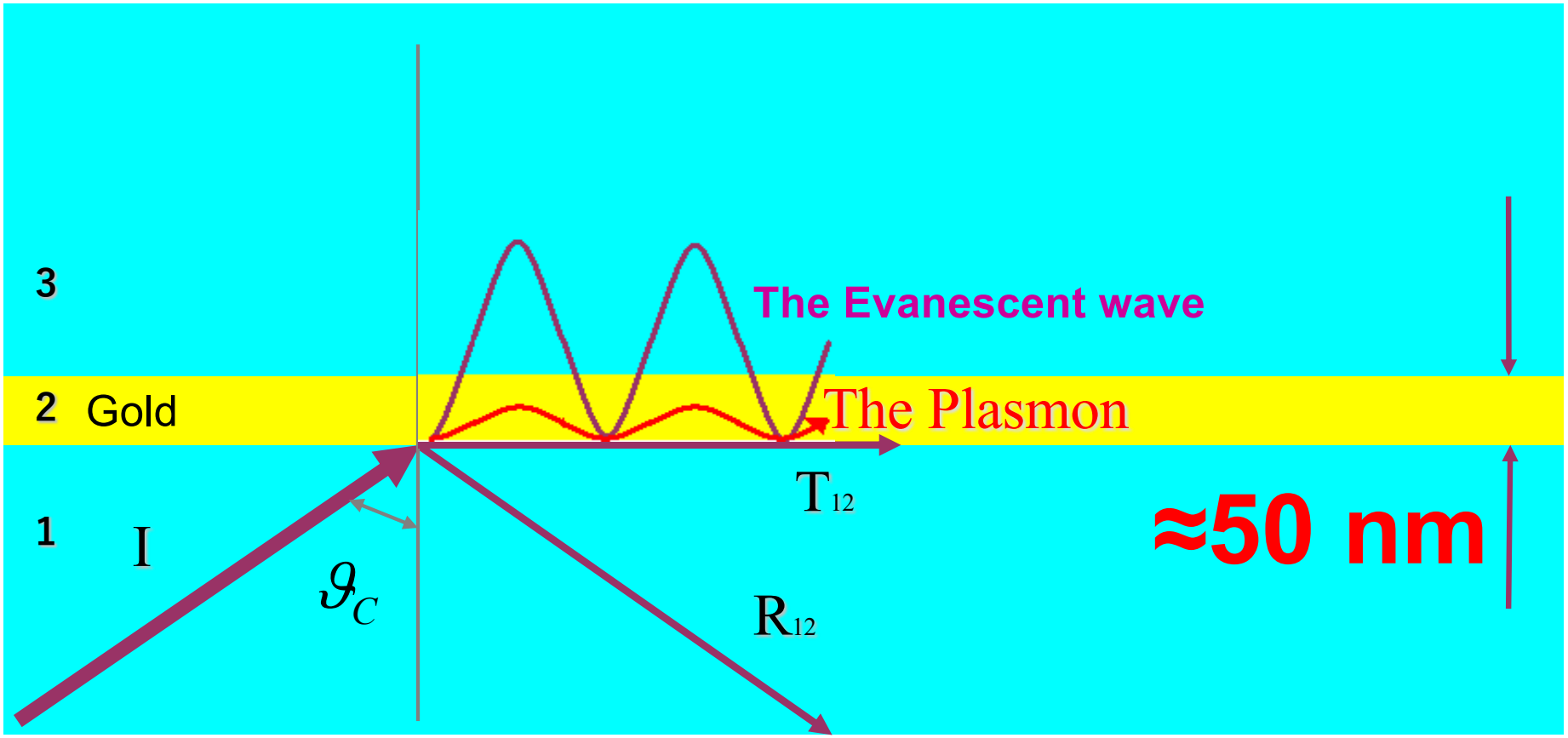

Perturbation of the Evanescent Wave

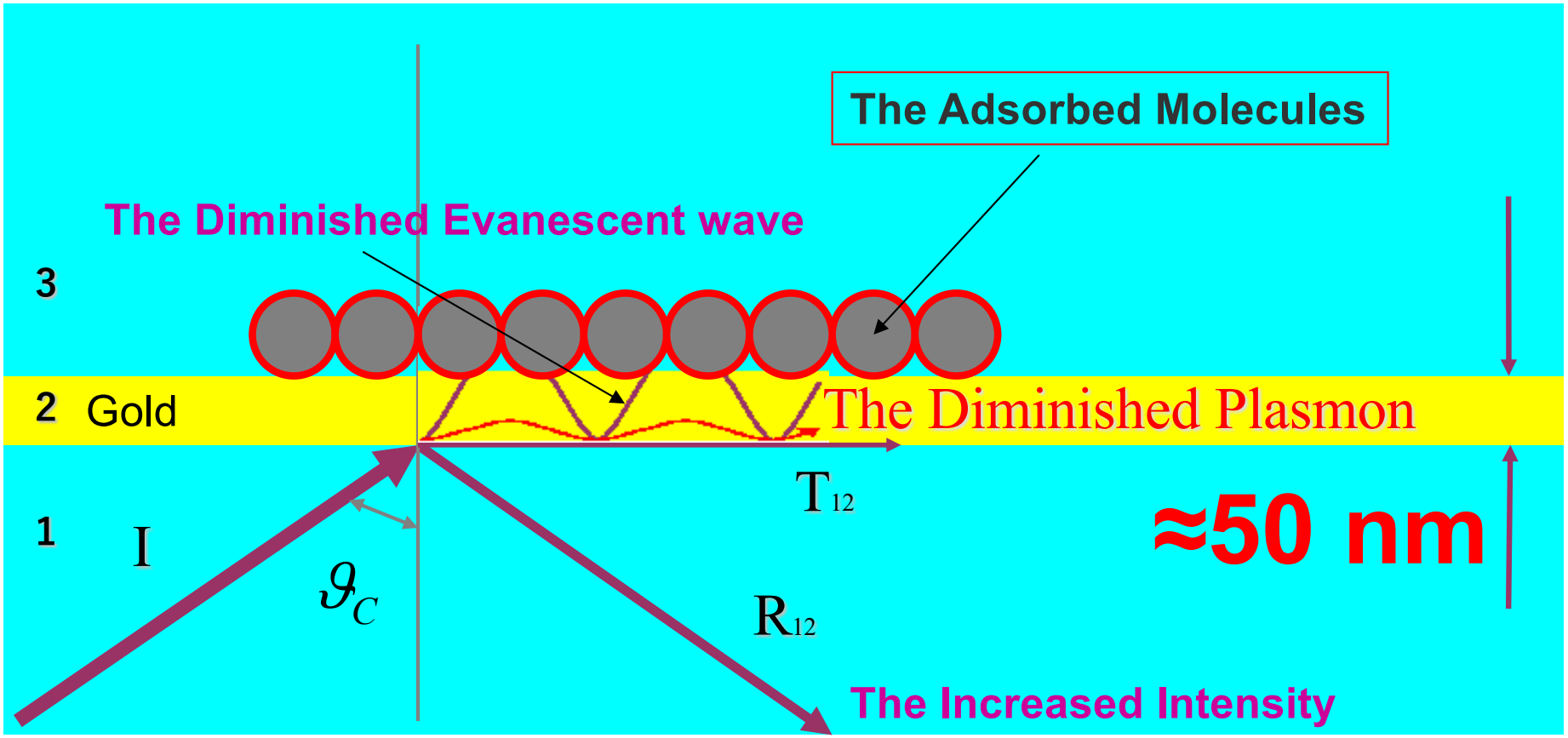

A Plasmon Resonance based Biosensor

BIACORE 3000

Working Principle

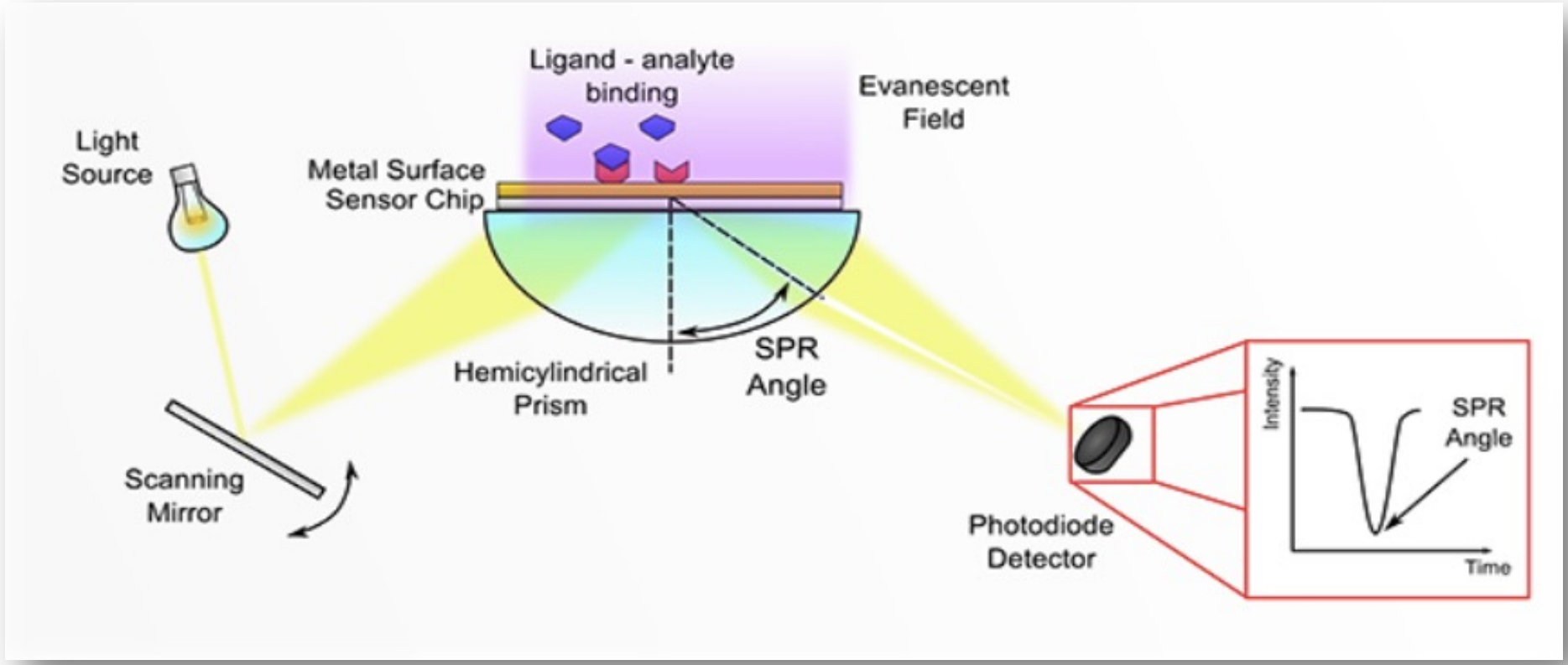

The presence of the complexes onto the gold surface will change the angle of resonance for the formation of the Surface Plasmon.

Characterization of Monoclonal antibodies

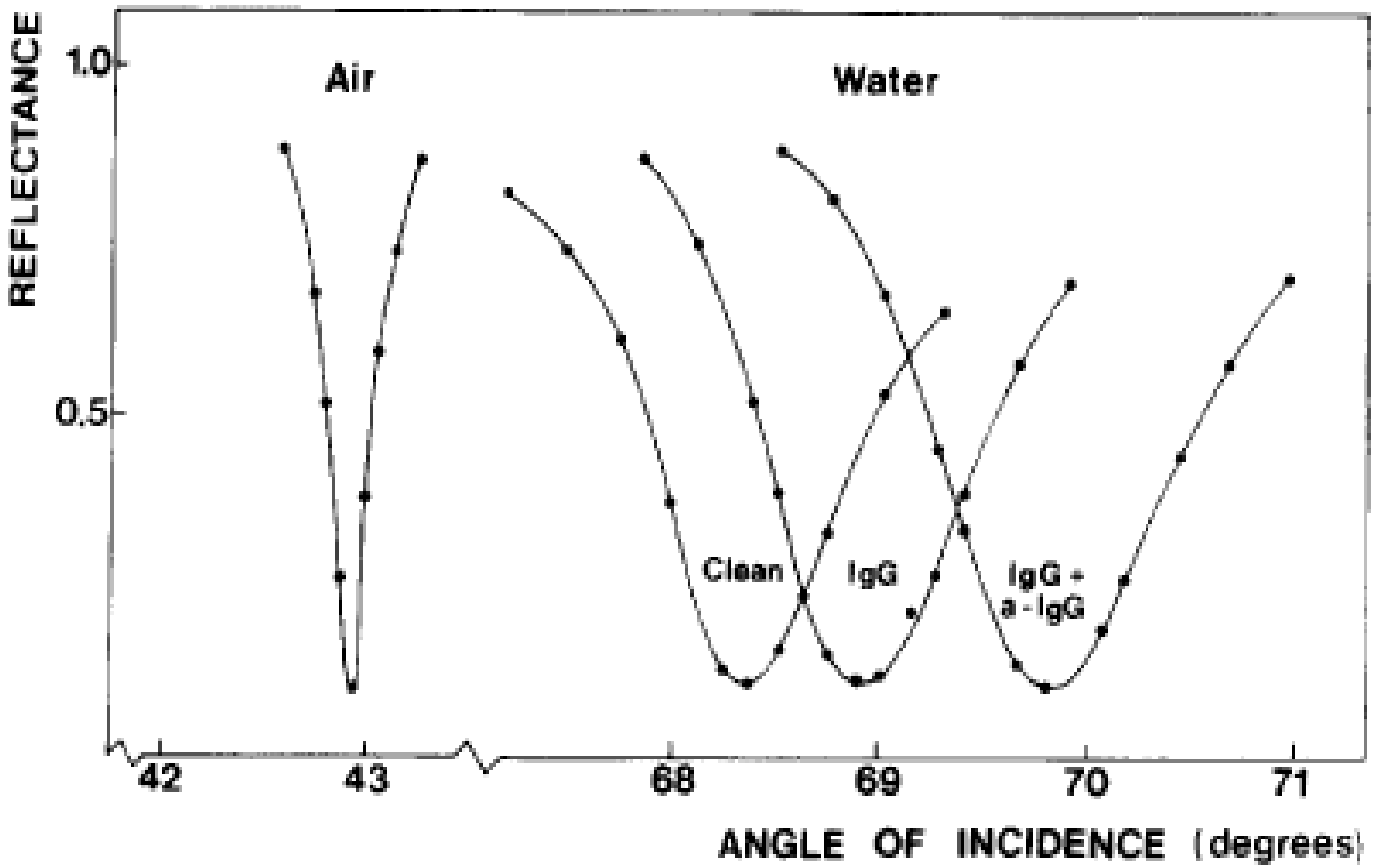

Bo Liedberg, et al, Biosensors & Bioelectronics 10 (1995) i-iv

Shift in the resonant angle to sense IgG adsorption

Kinetic Studies

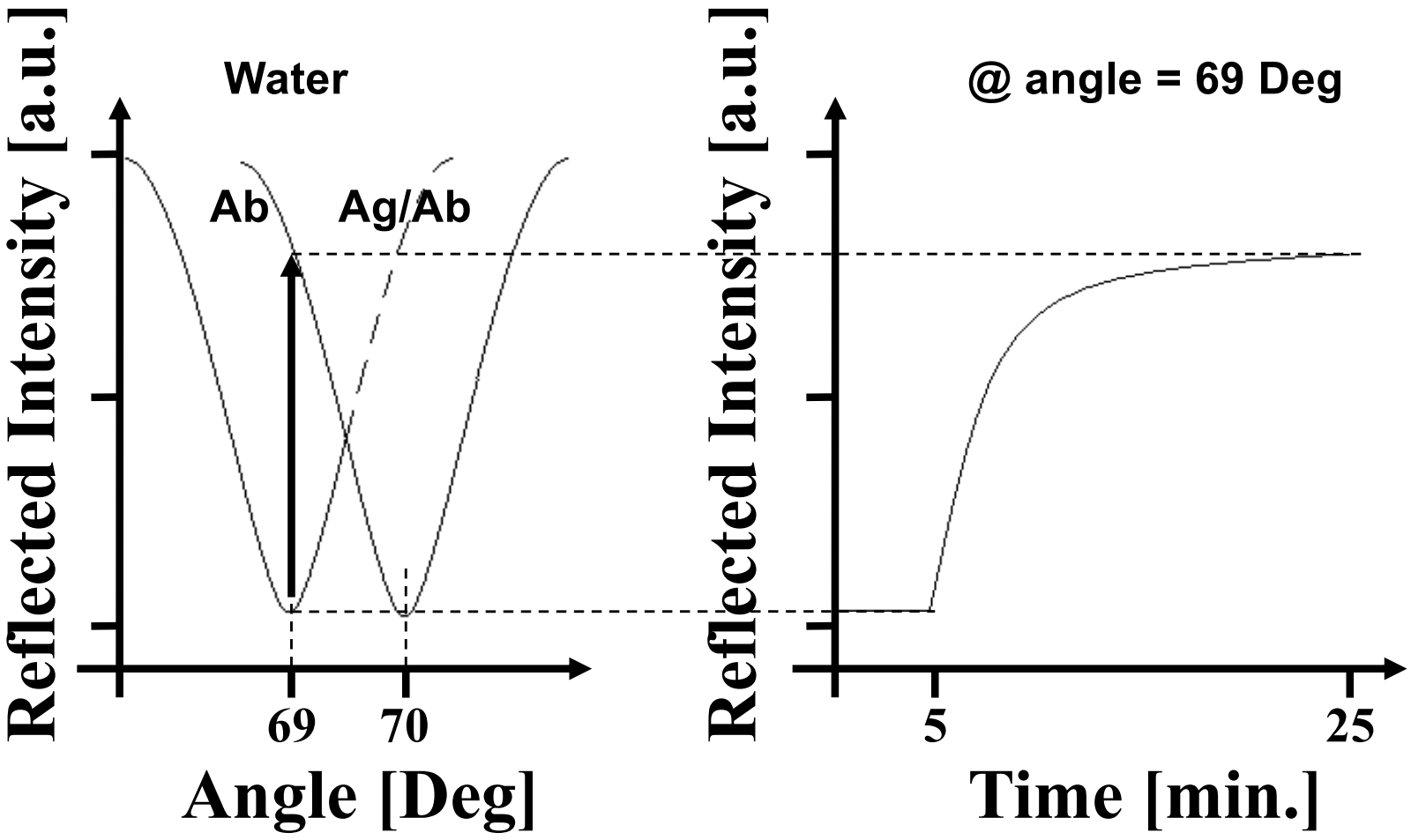

The kinetics could is reached by means of the change of the reflected intensity at fixed angle

Detection of Binding Events

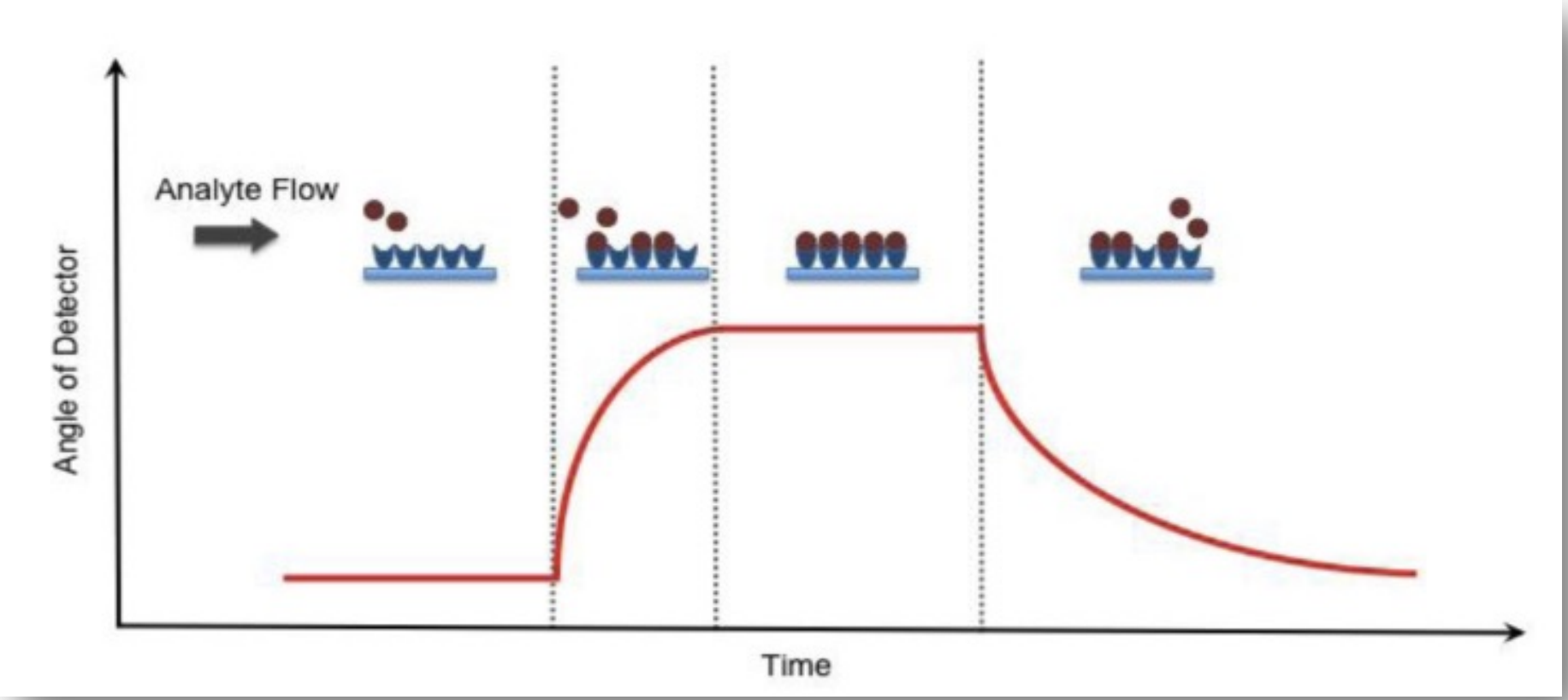

Molecular uptake as monitored by SPR

SPR on SAM

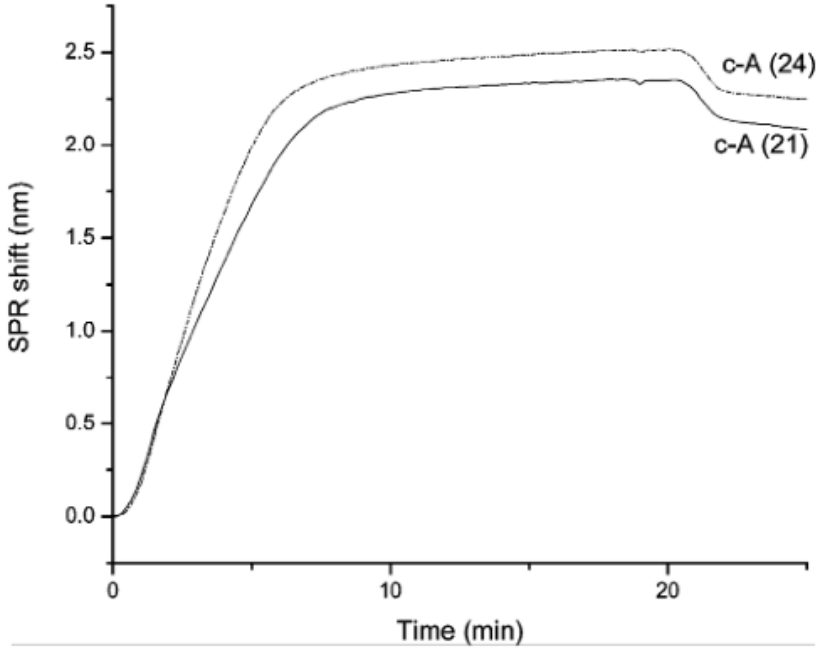

Figure 7. Comparison of the hybridization of a truncated complement (c-A 21) with the hybridization of the full-length complement (c-A 24). The ssDNA/OEG surface was prepared from a solution with a DNA mole fraction of 0.02.

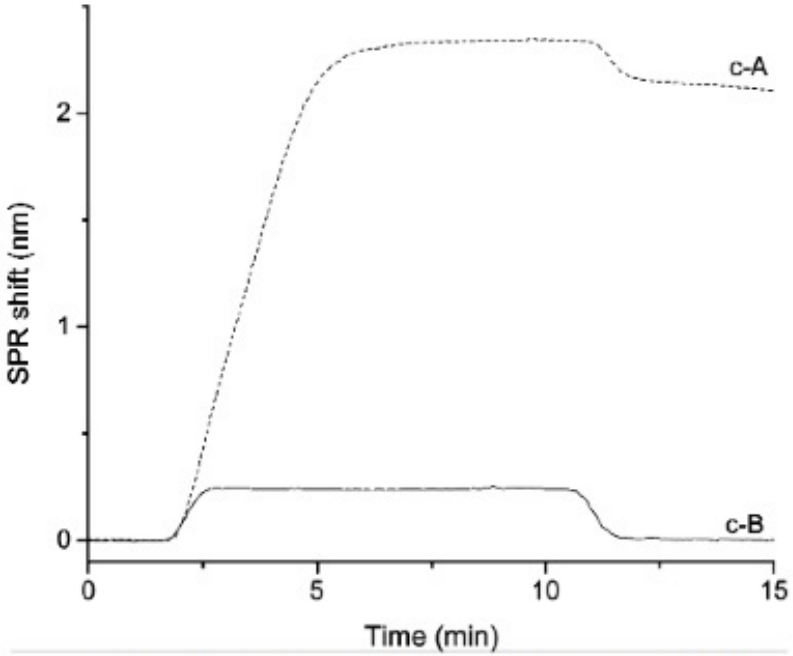

Figure 2. Control experiment to test DNA specificity. Both c-A and c-B were flowed over a sequence A ssDNA/OEG SAM, but only the complementary DNA hybridized. The ssDNA/OEG surface was prepared from a solution with a DNA mole fraction of 0.02.

Langmuir, Vol. 22, No. 10, 2006

DNA hybridization as monitored by SPR

How to characterize the Probes Immobilization?

We have seen what are the mechanisms of self-assembly!

How to monitor the self-assembly process?

How to check the film quality?

Four different Microscopies

1. Transmission Electron Microscopy (**TEM**)
2. Scanning Electron Microscopy (**SEM**)
3. Atomic Force Microscopy (**AFM**)
4. Scanning Tunneling Microscopy (**STM**)

All are Scanning Microscopies

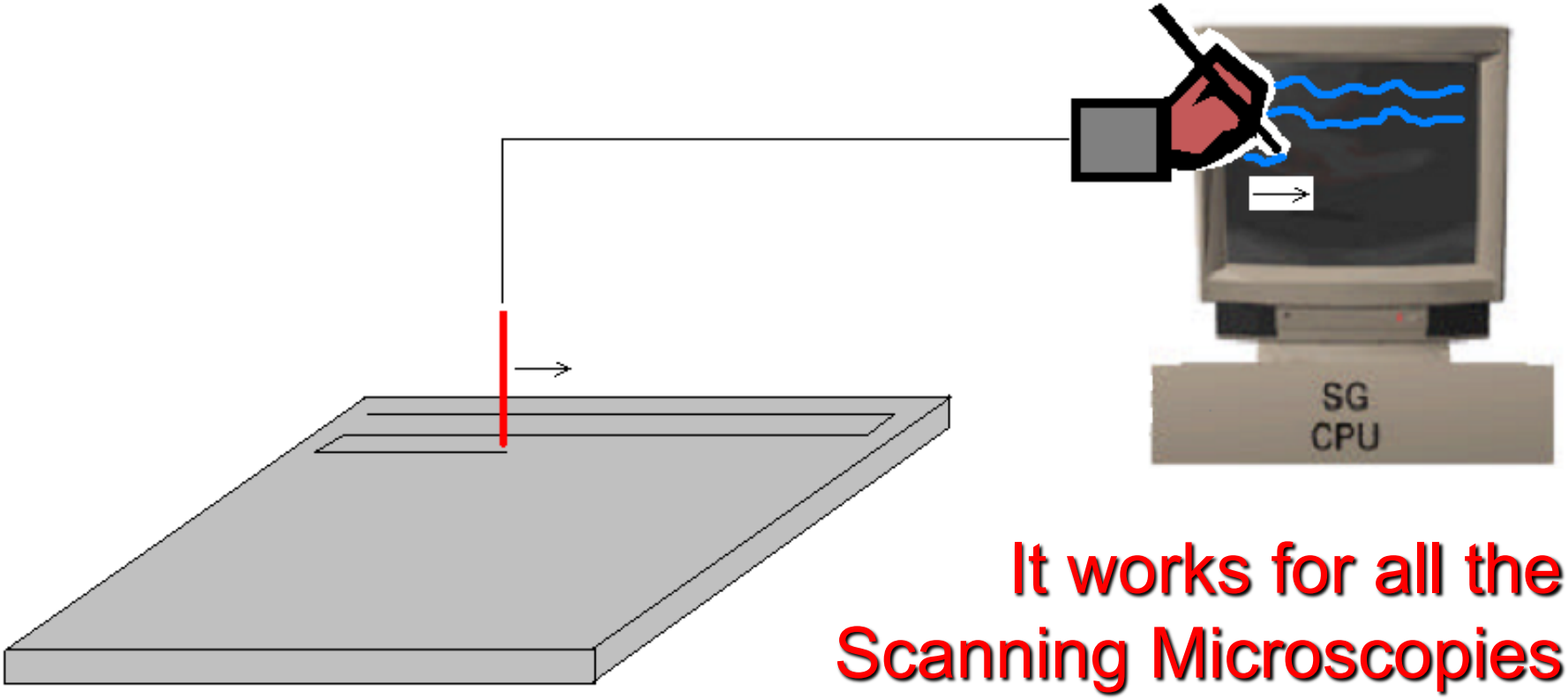

It works for all the Scanning Microscopies

The sample scanning generates an image visualized with computer graphic tools

SEM Microscopy

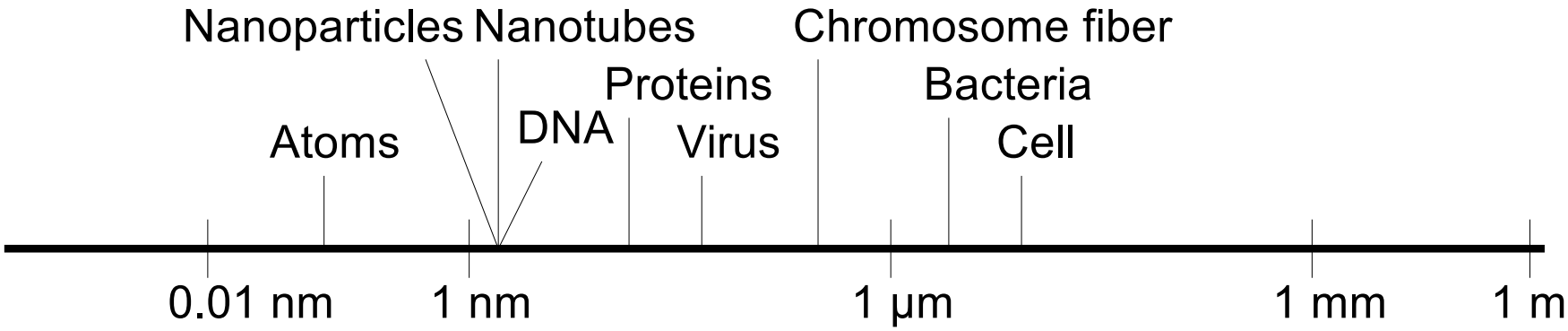

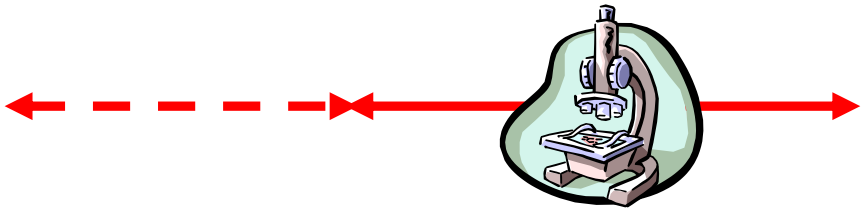

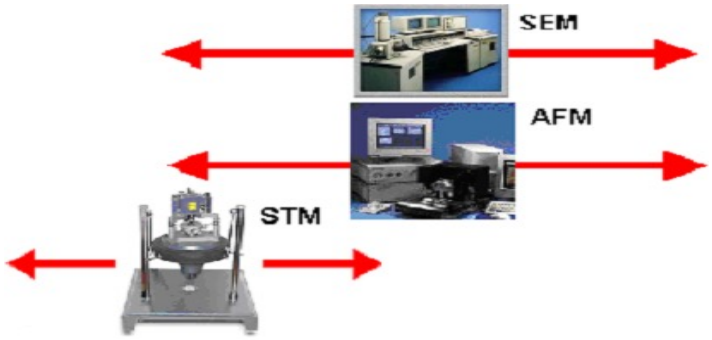

Electron Microscopies

Scanning Electron Microscopy

Transmission Electron Miscroscopy

Electron Microscopy Principle

[Emitted electrons from the same atom due to other electrons filling inner-shell vacancies created by scattered ones]

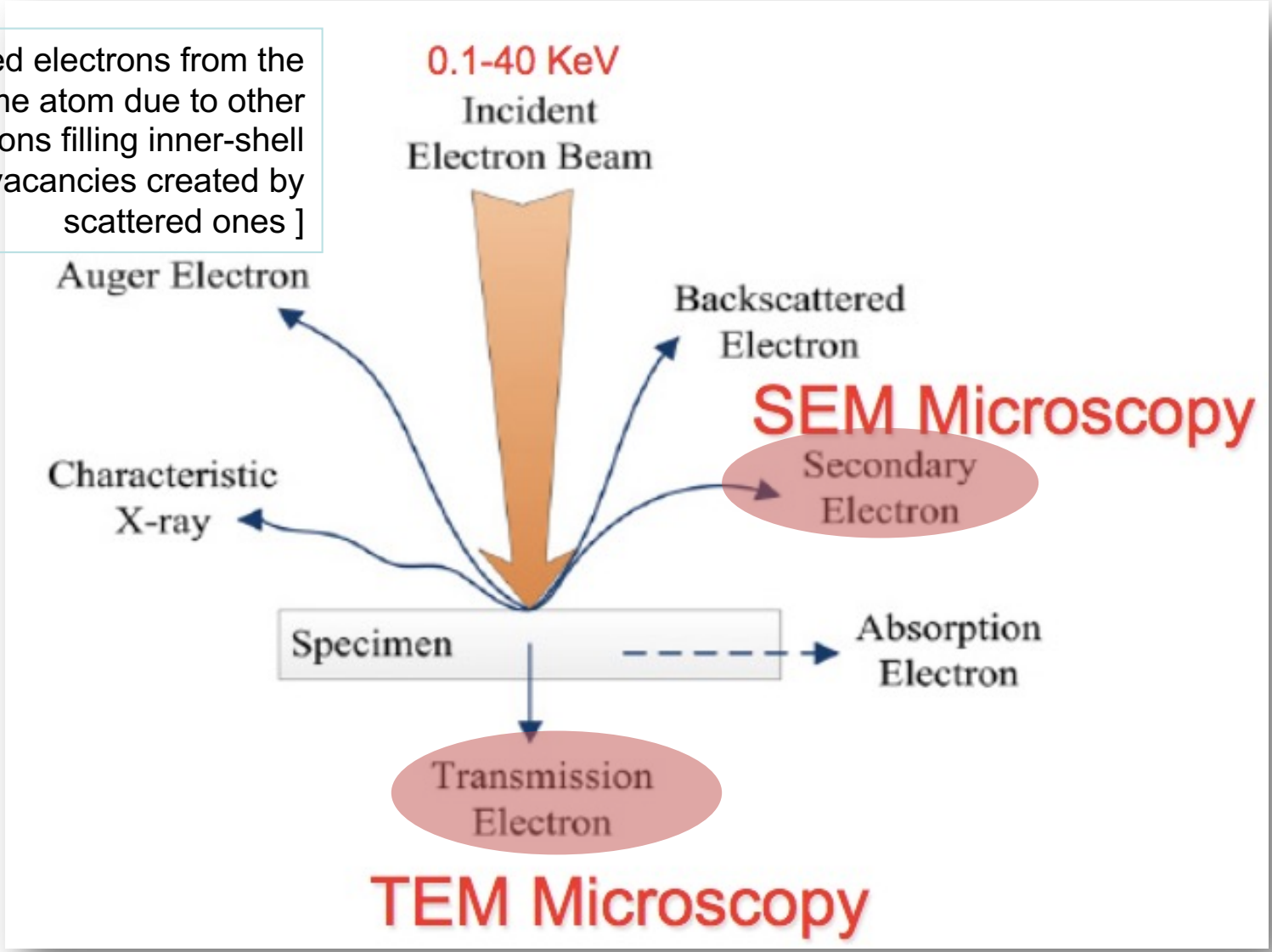

Electron Microscopies

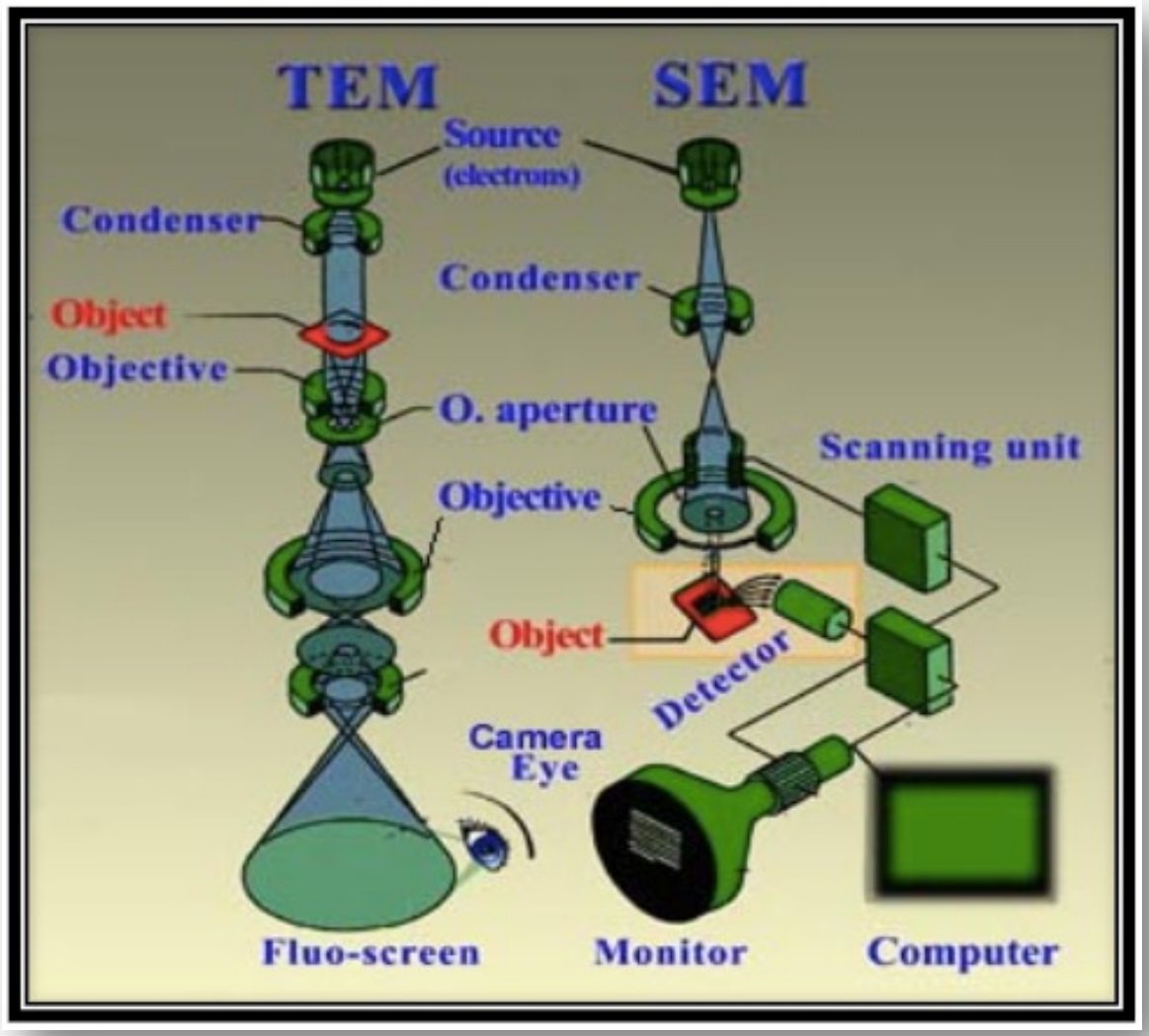

TEM Imaging

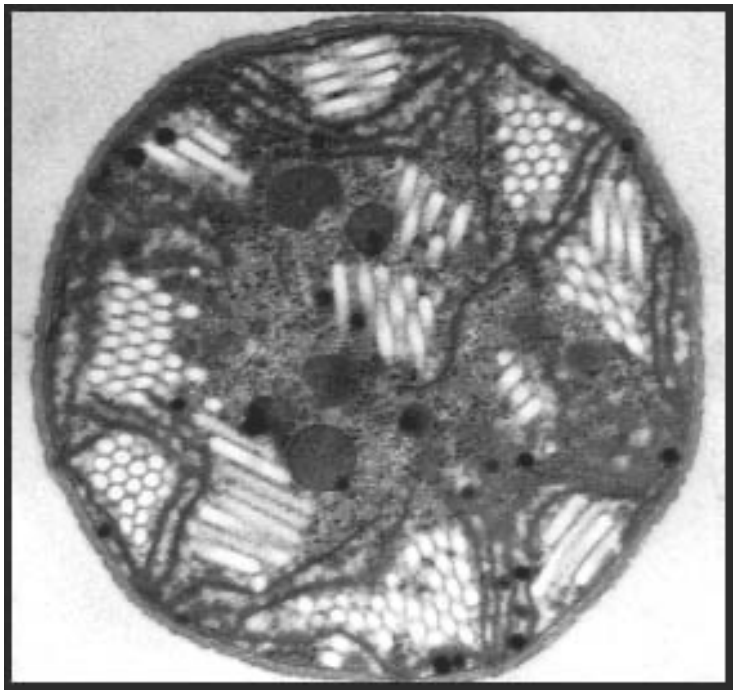

Cell of Cyanobacteria Microcystis by TEM

TEM Imaging

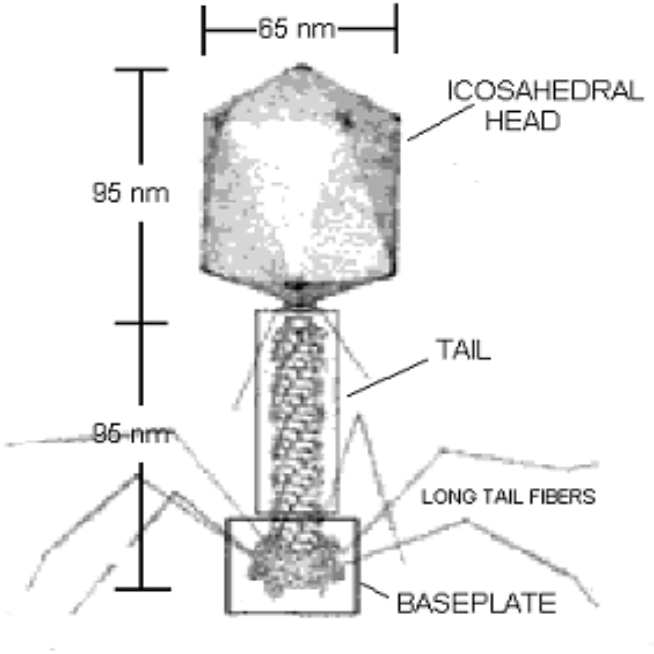

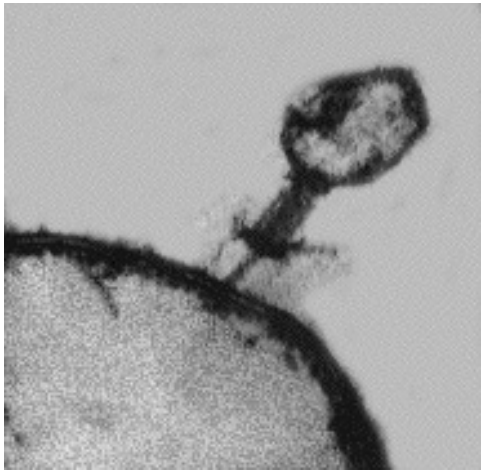

Virus T4 Bacteriophages

SEM Imaging

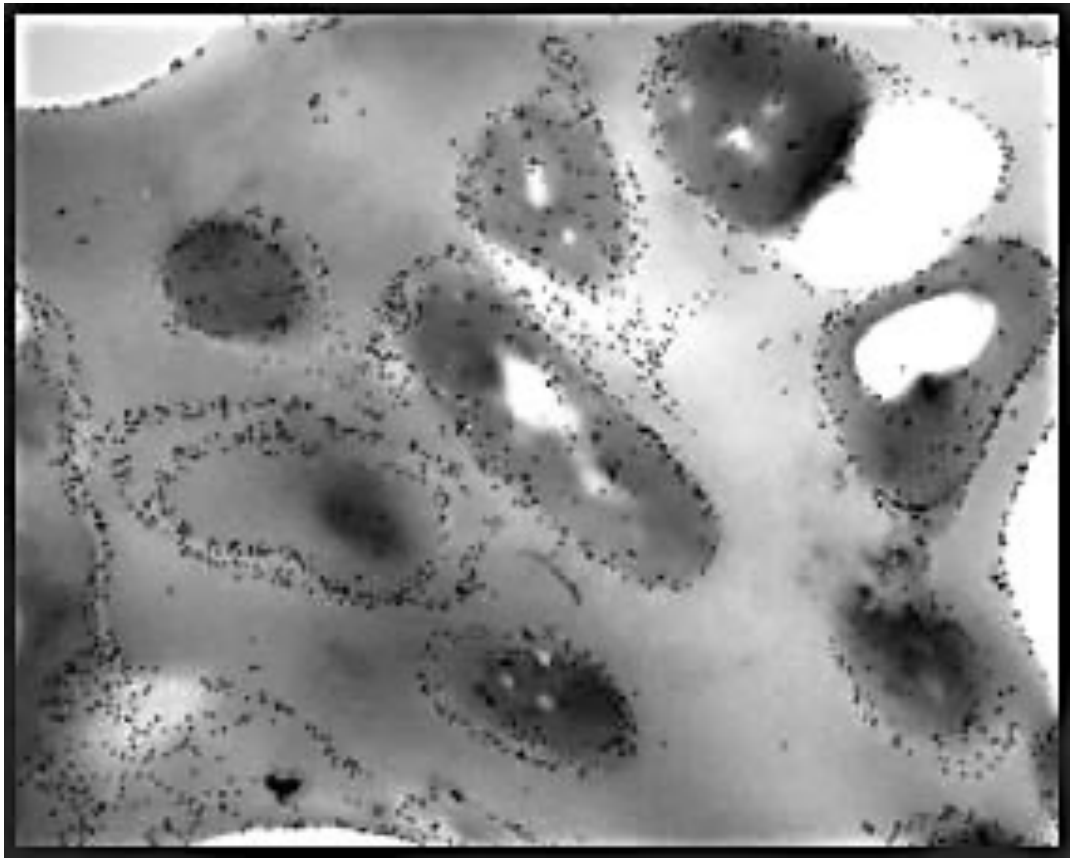

Antigens localized on the surface of bacteria cells

SEM Imaging

Isolated Chromatin (DNA-macromolecules including hystons and not-histons proteins) of about 30 nm and with small filament

SEM Imaging

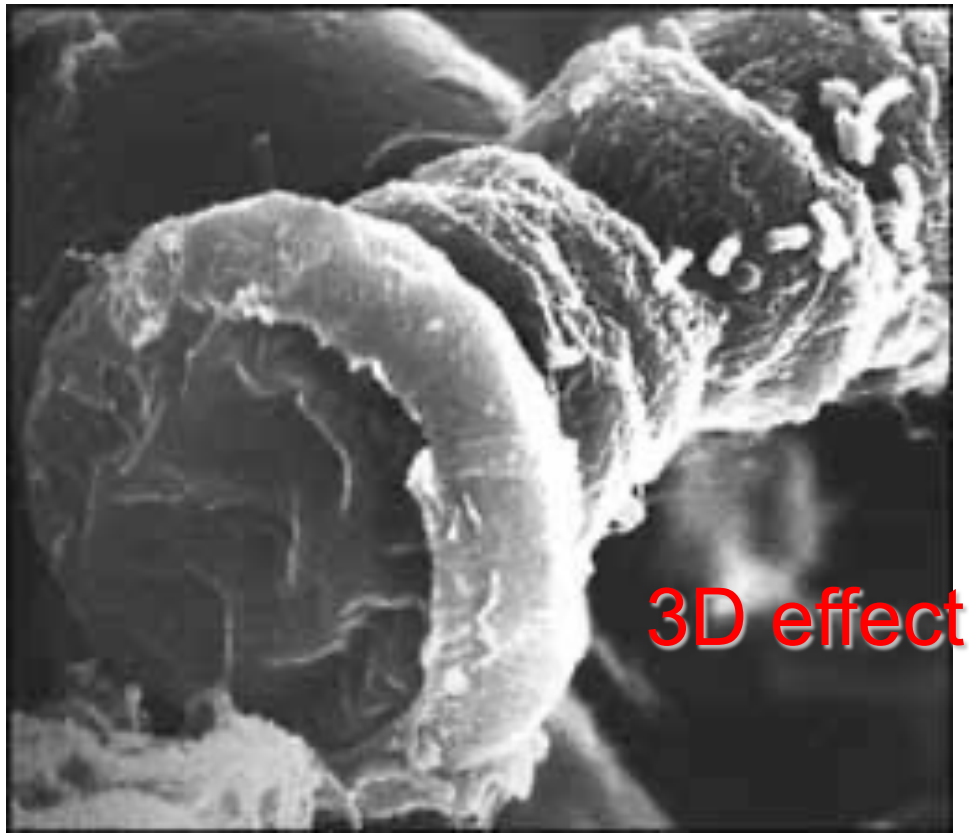

End part of Nodularia

(cyanobacteria in filament shape)

AFM detection principle

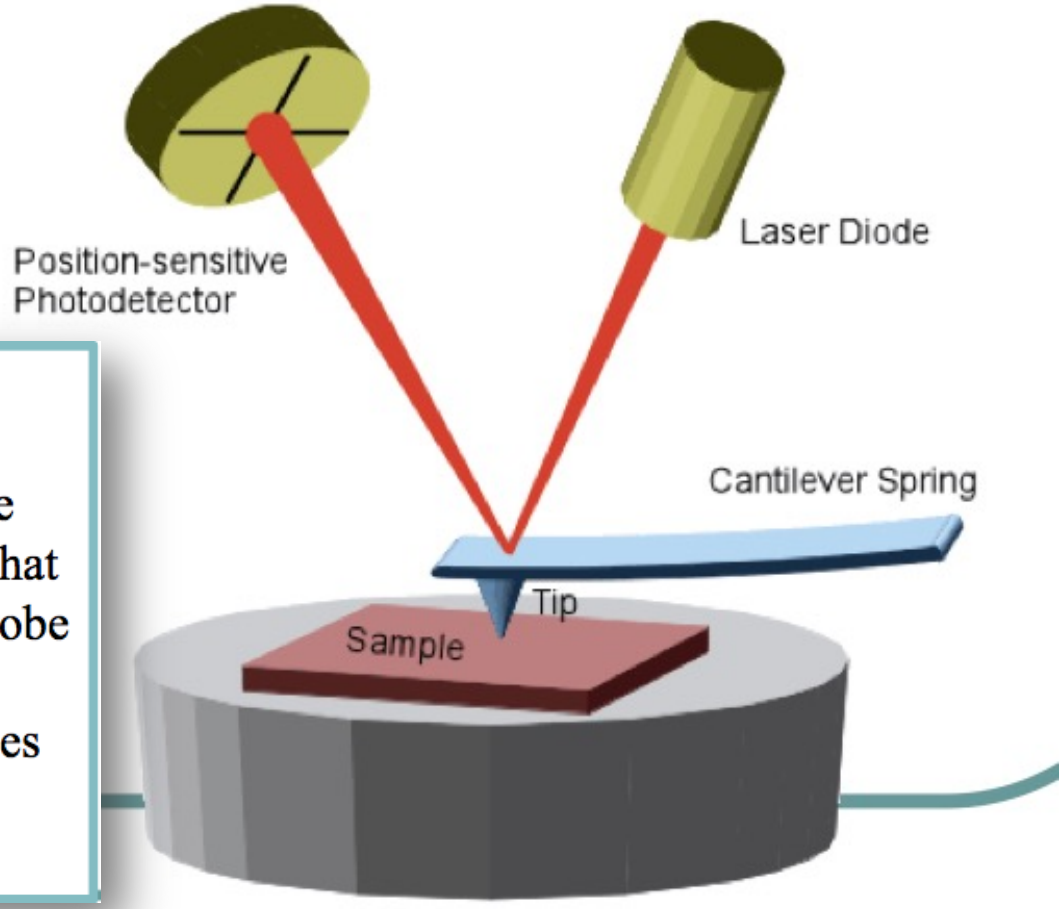

3 major abilities:

1. force measurement between probe-sample
2. imaging from forces that sample imposes on probe (3D, pseudocolor)
3. manipulation use forces to change sample properties

Detection principle is obtained by monitoring the bending of the cantiliver that host the tip

AFM Tip fabrication

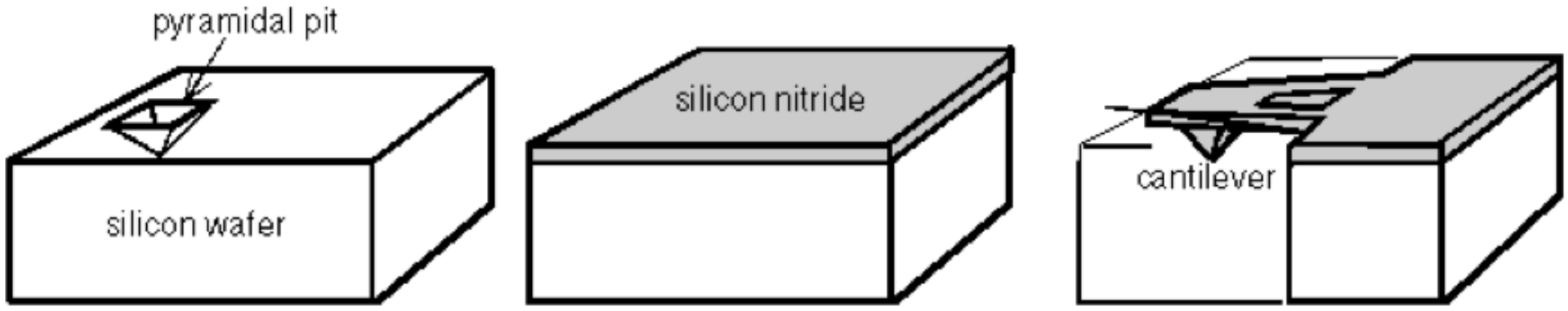

Pit etching in Si Si_3N_4 coating Si underetching

AFM tips are typically sculpted on silicon wafers

SEM on Silicon nitride probes

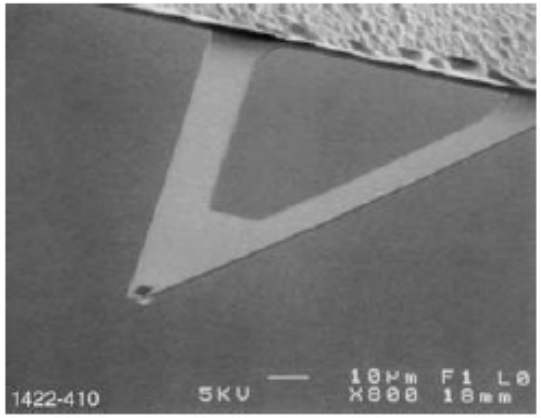

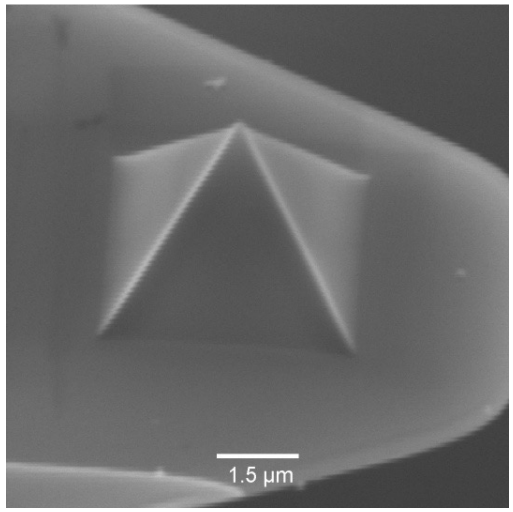

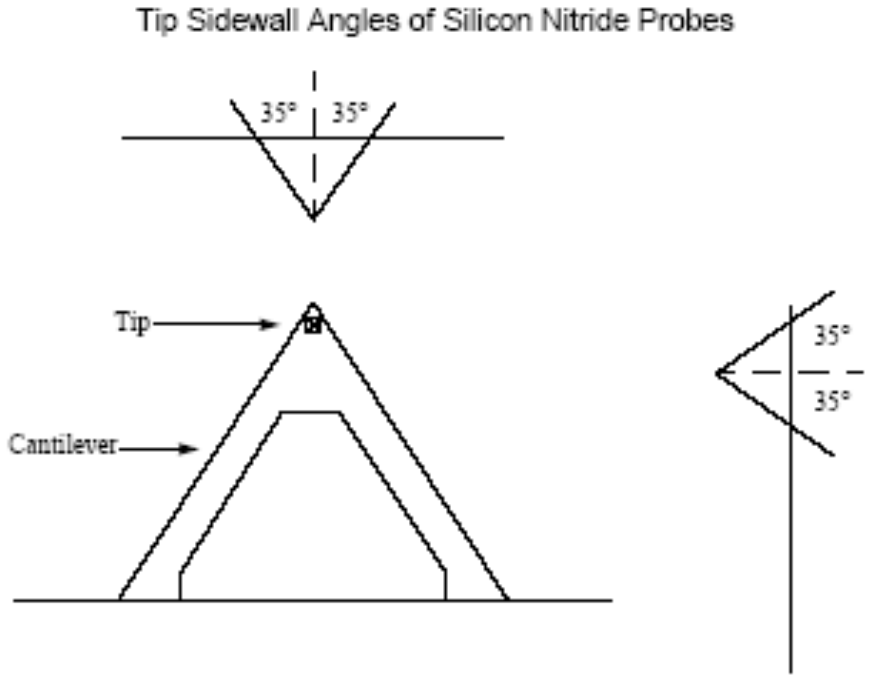

(credit by Cambridge University)

Optics versus AFM

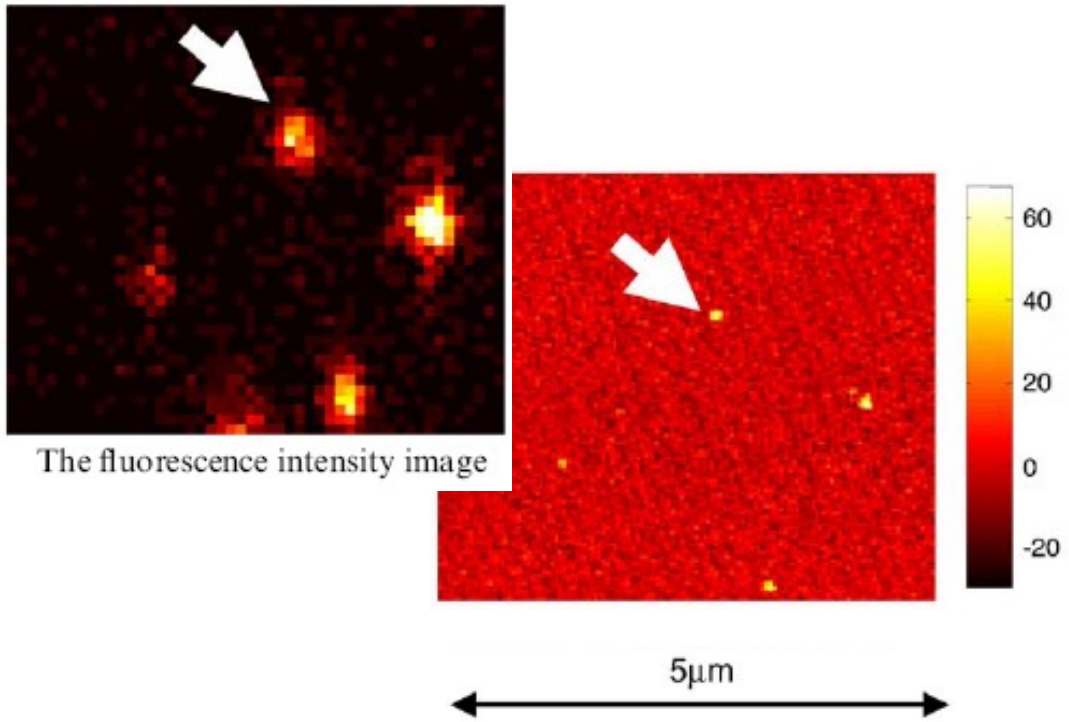

Fluorescent Nanoparticles with average size of about 40 nm

AFM Imaging

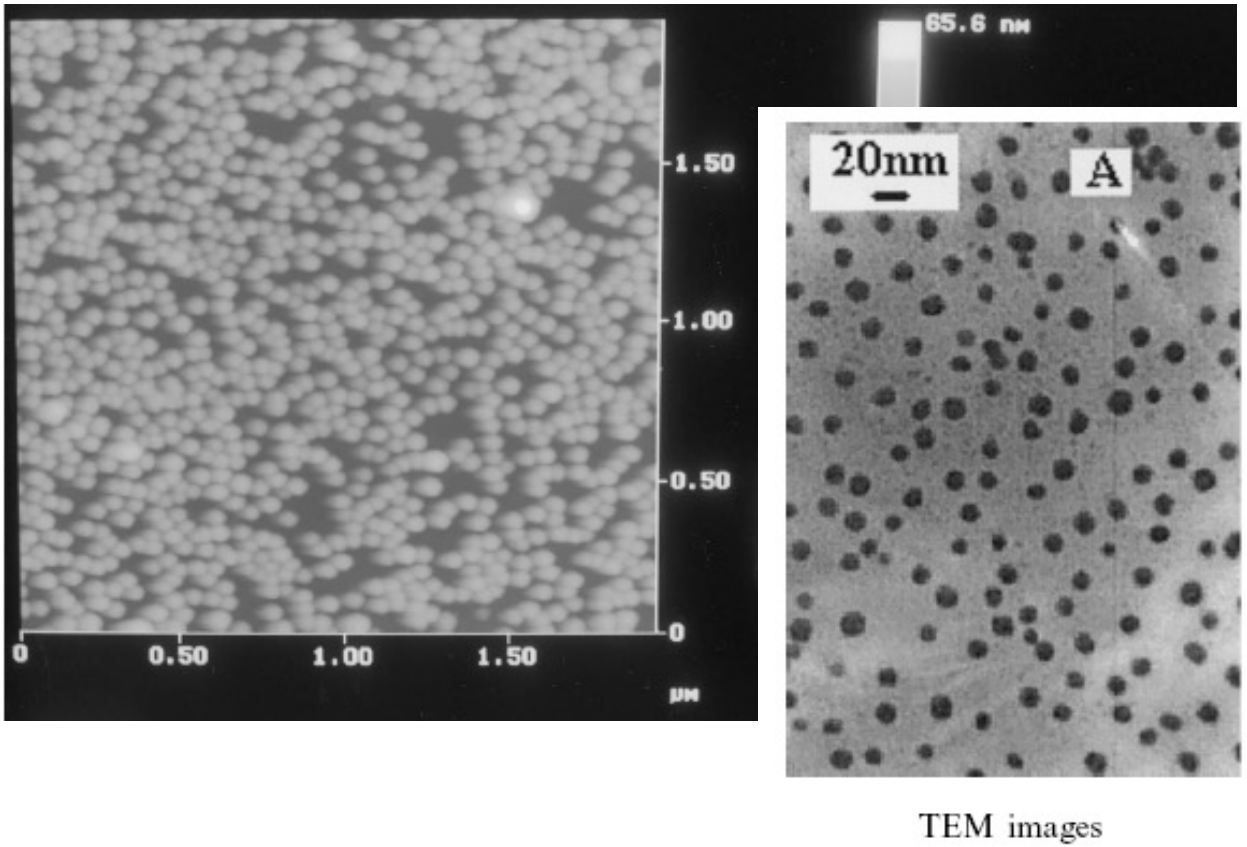

TEM images

Gold nanoparticles made off gold core and a thiols-shell to stabilize the particle

AFM Imaging in Air

dx.doi.org/10.1021/bm301063m | *Biomacromolecules* 2012, 13, 3503−3509

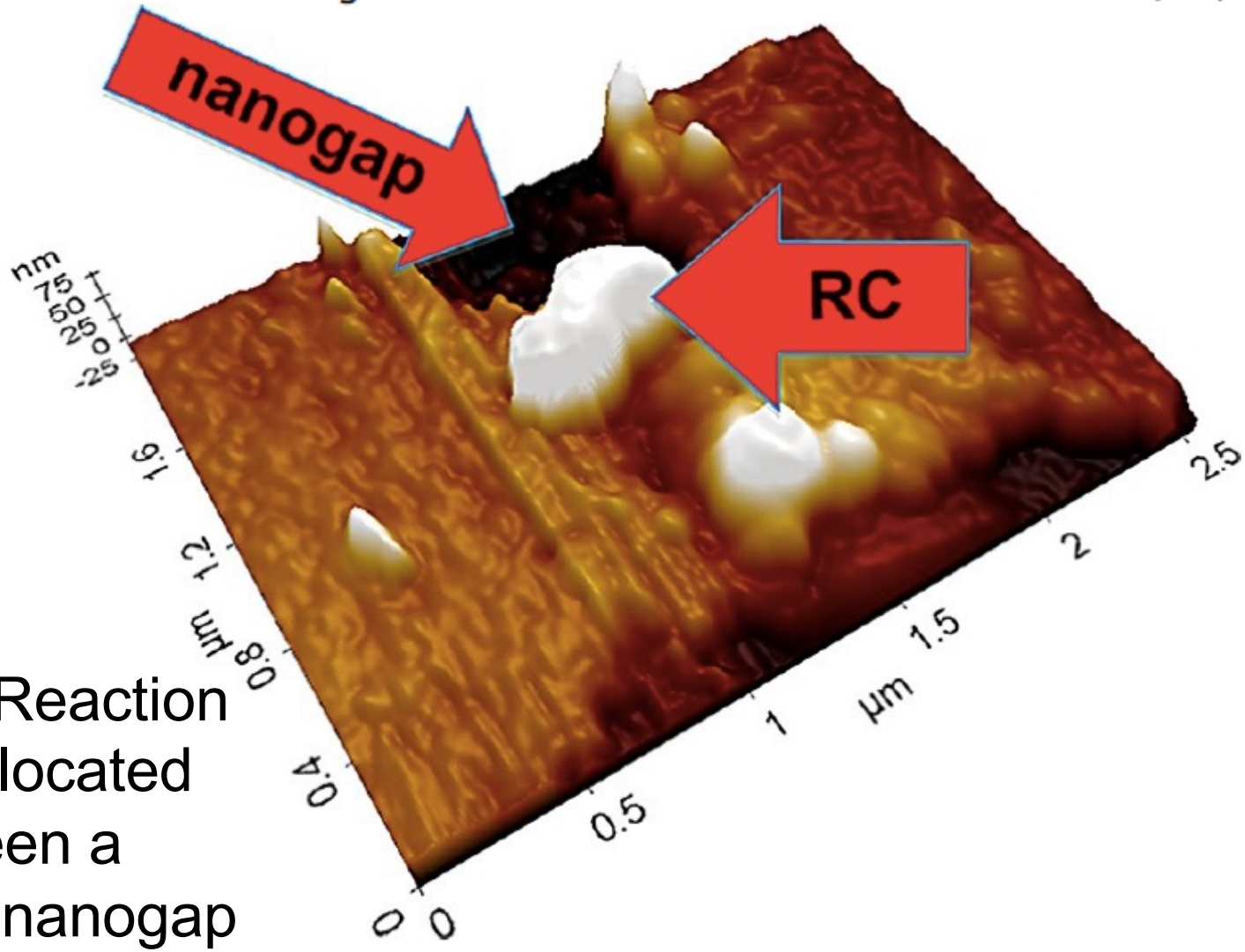

A protein (Reaction Center) located in between a metallic nanogap

AFM in liquid

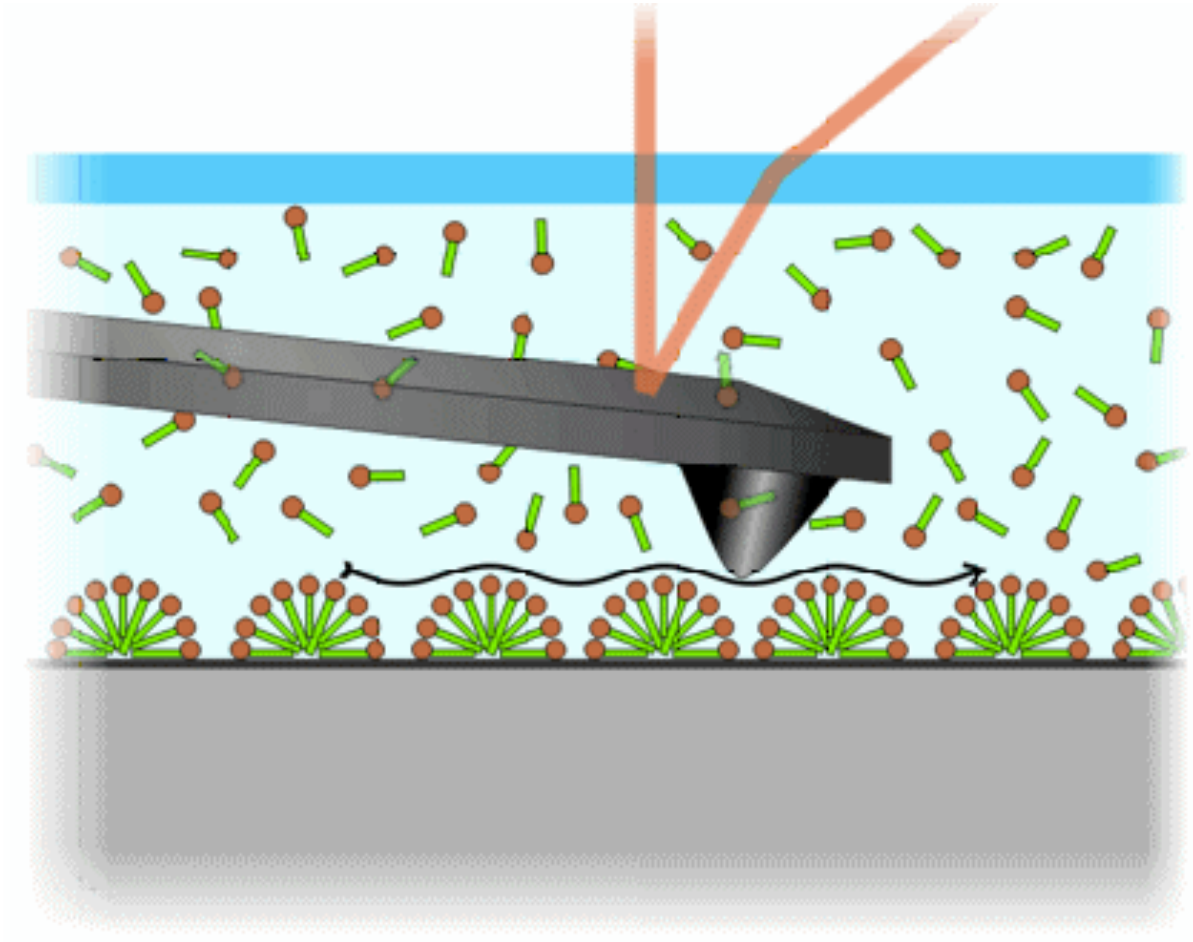

AFM is also used fully in water for imaging typically biological systems in their native environments

AFM Imaging in liquid

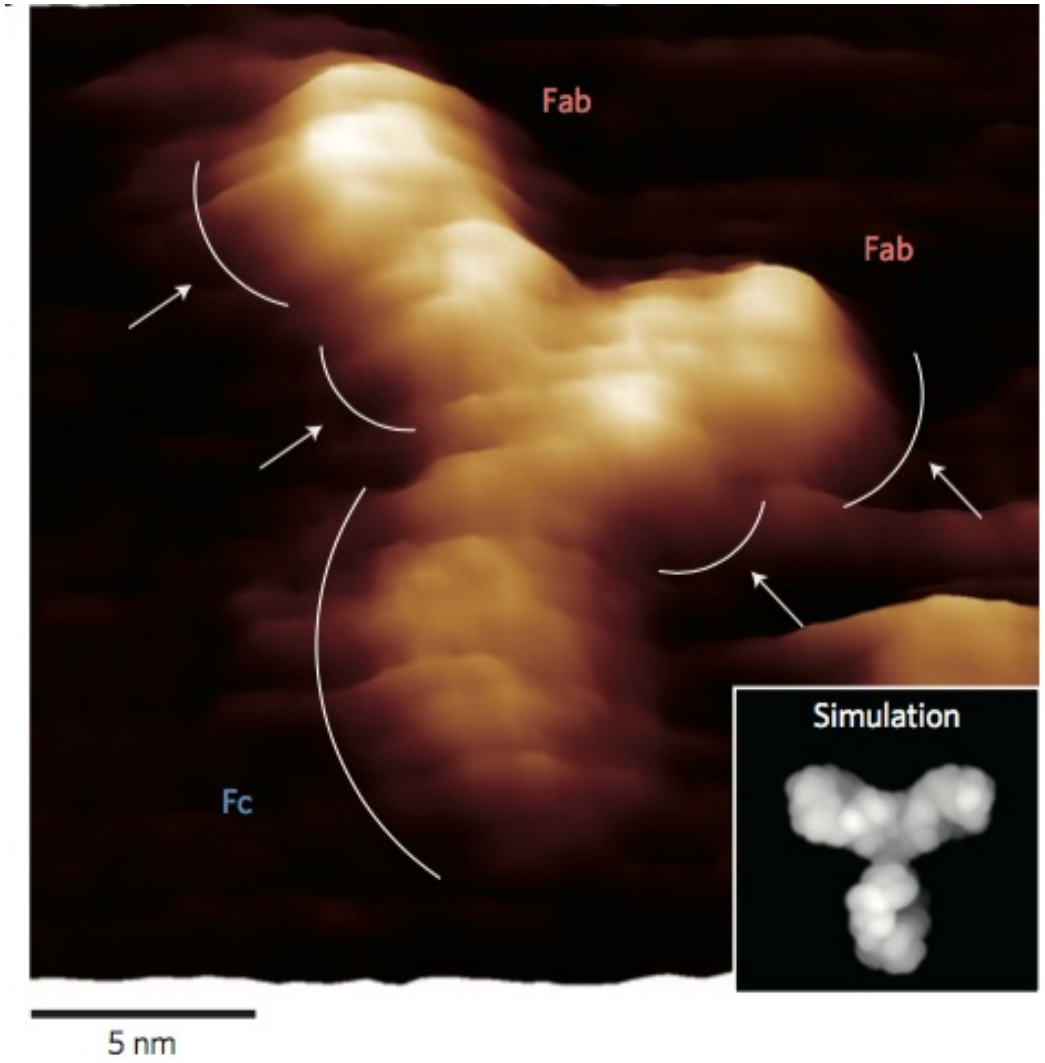

AFM imaging on Antibodies

Dense nanostructure arrays

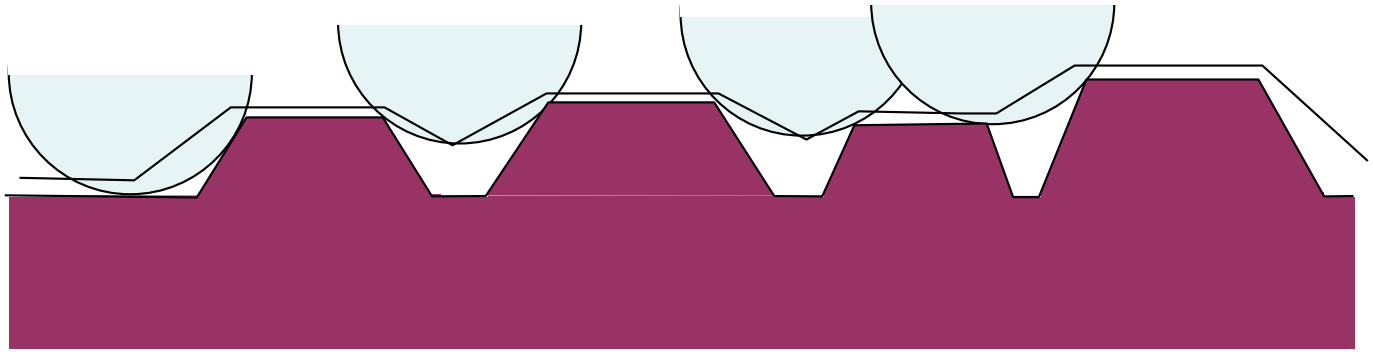

For densely packed features the tip size can also cause errors in determining the height of the islands, or the overall appearance of the surface

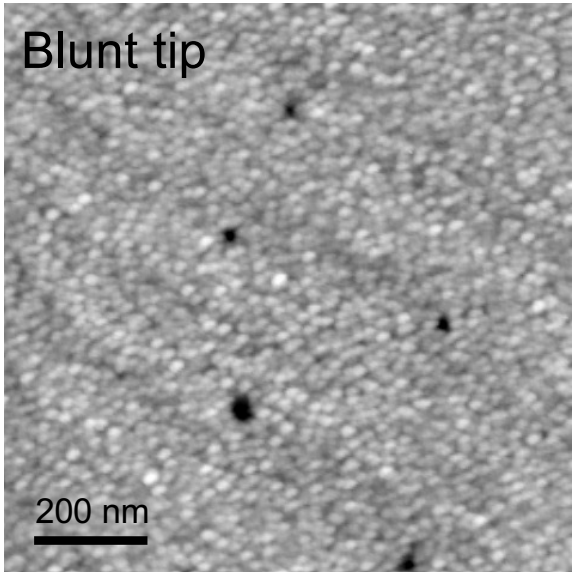

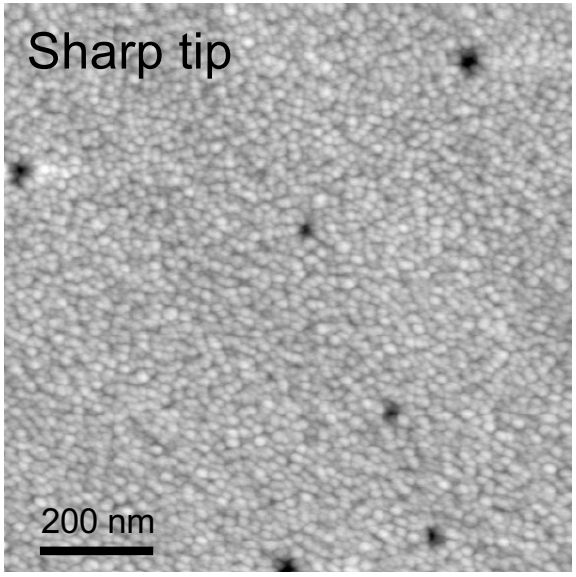

(credit by Cambridge University)

STM Microscopy

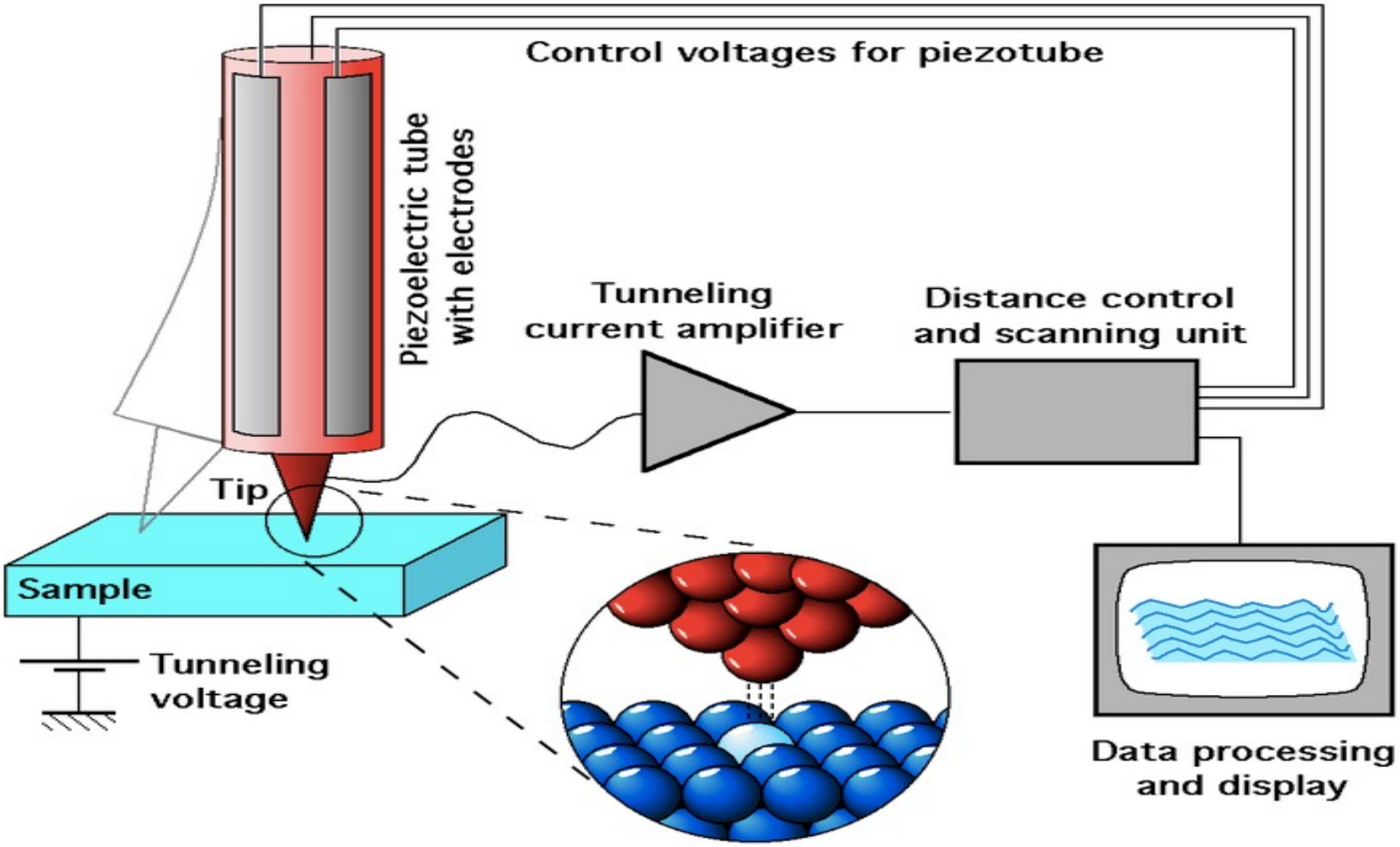

The STM Microscopy is based on tunneling currents as established in between the tip and the sample

STM Microscopy

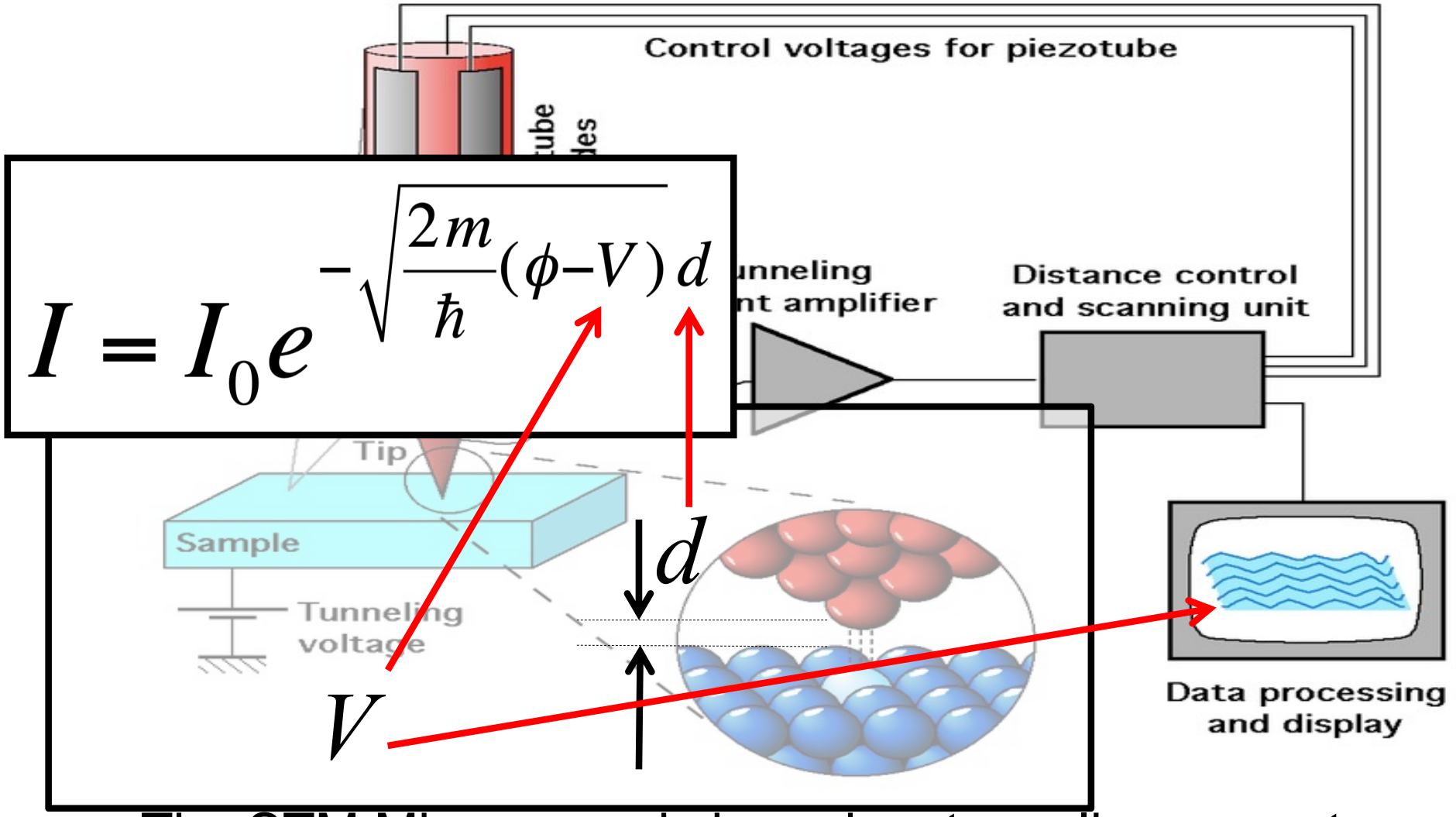

The STM Microscopy is based on tunneling currents as established in between the tip and the sample

STM imaging

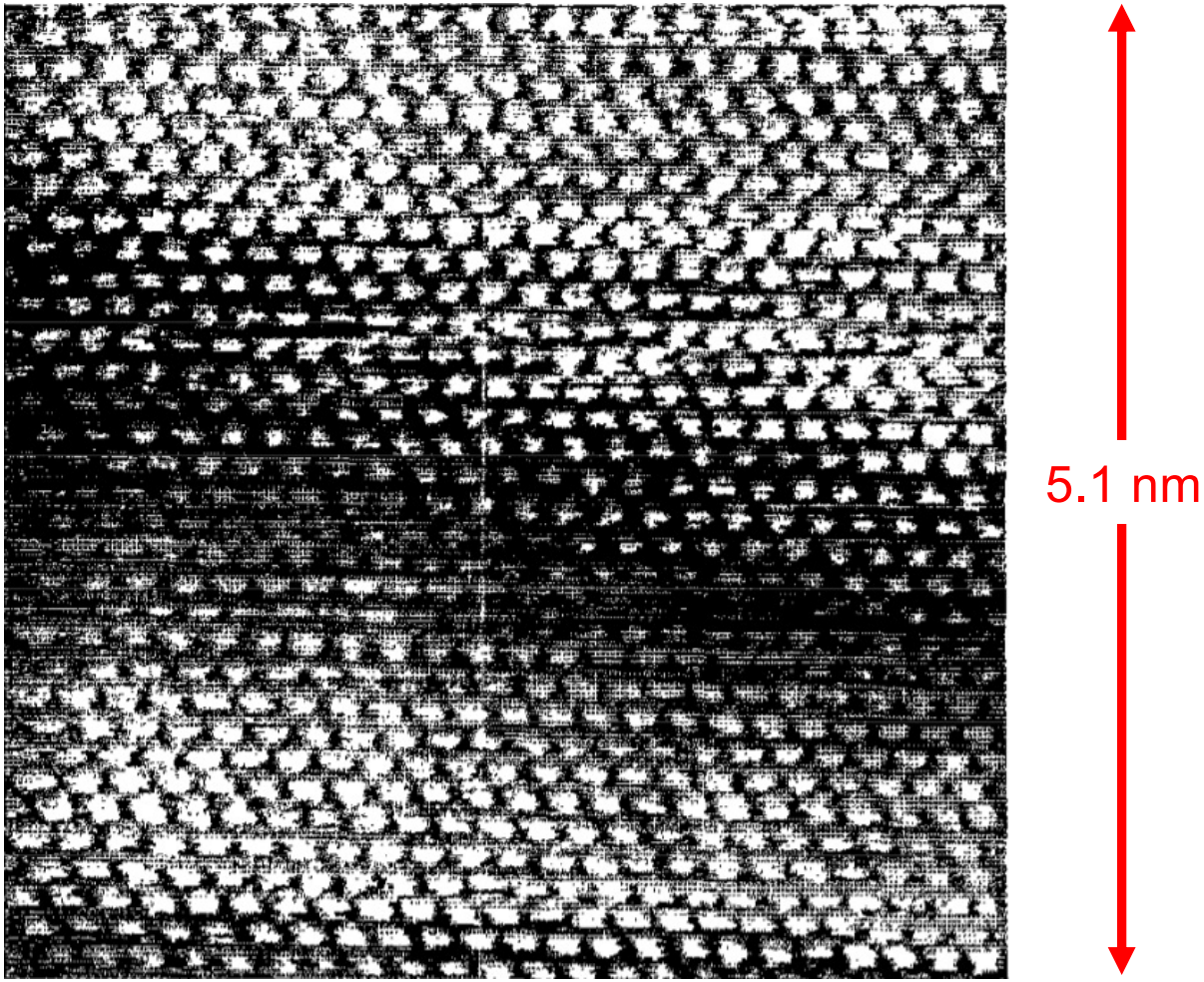

Carbon atoms in the lattice structure of the highly oriented pyrolytic graphite. Image by STM in air.

STM imaging

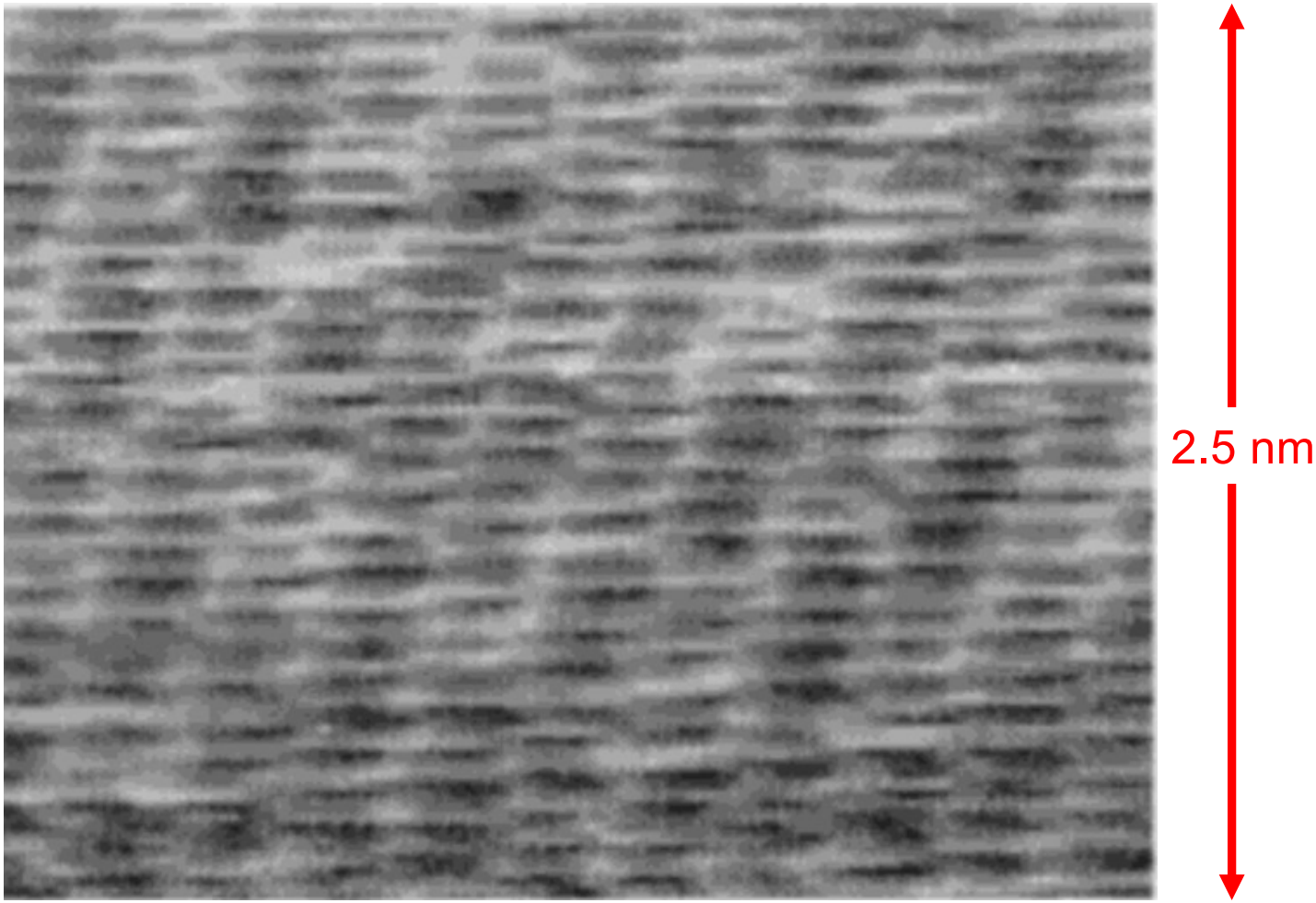

Organic thiols self-assembled onto highly oriented pyrolytic graphite. Image by STM in air.